Pergamon

Int. J. Solids Structures Vol. 31, No. 16, pp. 2167–2193, 1994

0020–7683/94 $7.00 + .00

0020–7683(94)E0021–M

AN ANALYSIS OF NON-PLANAR CRACK GROWTH UNDER MIXED MODE LOADING

G. XU, A. F. BOWER† and M. ORTIZ
Division of Engineering, Brown University, Providence, RI 02912, U.S.A.

(*Received* 24 *August* 1993; *in revised form* 24 *January* 1994)

Abstract—A method is presented for calculating stress intensity factors at the tip of a slightly wavy three-dimensional crack. The solution is used to calculate the direction of propagation of an initially planar semi-infinite crack, which is subjected to uniform remote loading. In particular, the combinations of remote load which cause the crack to deviate from its original plane are found. For the particular case of a two-dimensional crack subjected to combined mode I and mode II loading, we recover the results of Cotterell and Rice [1980, *Int. J. Fract.* **16**(2), 155]. For a crack loaded by combined mode I and mode III loading, it is shown that there is a critical ratio of K_{III}/K_I which causes the crack to deviate from its original plane. The influence of T-stresses, which act parallel to the crack plane, is also investigated. Finally, the predictions of the perturbation theory are compared with full-field numerical simulations which predict the path of a crack propagating under mixed mode remote loading.

1. INTRODUCTION

When a crack propagates through a brittle solid, if often follows a tortuous path. Inhomogeneities such as grain boundaries and second phase particles tend to deflect cracks; local variations in residual stress within the material have a similar effect. In addition, if the loading applied to the solid induces mixed-mode stress intensity factors on the crack tip, then the crack generally deviates from its initial plane. The strength of the solid may depend strongly on the path followed by the crack, for several reasons. For example, if the crack meets reinforcing particles, they may cause the crack to arrest and so enhance toughness. The crack path also determines the roughness of the crack faces. If the roughness is sufficiently large, the crack faces may contact. The resulting friction forces between the crack faces tend to reduce the crack tip stress intensity factors and so improve the apparent toughness of the material. This effect is thought to be particularly important in mixed mode I/mode III fracture (Suresh and Tschegg, 1987; Tschegg and Suresh, 1988; Suresh *et al.*, 1990).

It has been shown that the principles of linear elastic fracture mechanics can be used to predict the path of a crack in a brittle solid. A number of authors have investigated the behavior of a crack subjected to mixed mode I and mode II loading. Experiments show that if a planar crack is loaded by a combination of K_I and K_{II}, it initially branches at a characteristic angle, and thereafter approaches a trajectory which is perpendicular to the maximum principal stress (Radon *et al.*, 1977). Various criteria have been proposed to predict the angle at which the crack kinks. Examples include the maximum hoop stress criterion (Erdogan and Sih, 1963; Williams and Ewing, 1972; Finnie and Saich, 1973; Ewing and Williams, 1974; Ewing *et al.*, 1976), the maximum strain energy release rate criterion (Cotterell, 1965; Palaniswamy and Knauss, 1978) and the stationary Sih energy density factor (Sih, 1973, 1974). The criteria predict slightly different angles for the initial kink but they all predict that, once the kink has initiated, the trajectory of the crack is such that $K_{II} = 0$ at the crack tip. To predict the crack path, one must find a crack shape that satisfies $K_{II} = 0$ during all stages of crack growth. One approach to this problem is to calculate the stress intensity factors for the crack using a numerical method and to extend the crack incrementally. The direction of each increment in crack length is chosen so as to

† Author to whom correspondence should be addressed.

satisfy the appropriate fracture criterion. Fleck (1991) has used this technique to calculate the path of arrays of cracks subjected to a range of remote loads. An alternative approach to predicting crack trajectories in two dimensions has been developed by Cotterell and Rice (1980). By perturbing the complex potentials which generate the stress fields around a planar crack, they found remarkably simple expressions for the stress intensity factors for a slightly wavy two-dimensional crack. Similar perturbation methods have also been used by several other authors (Banichuk, 1970; Goldstein and Sagalnik, 1974; Karihaloo *et al.*, 1981; Sumi *et al.*, 1983). The results of these calculations have been used to predict the conditions necessary to cause a planar crack to deviate from is initial plane. Provided that the crack trajectory does not deviate too far from a planar configuration, it is also possible to find closed form solutions for the crack path.

The analogous three-dimensional problem of a crack subjected to mixed mode I and mode III loading is not as well understood. Experiments show that this type of loading can cause cracks to propagate along a wavy path. For example, if a circumferentially pre-cracked bar is fractured by a combination of torsion and tension, then it is found that the macroscopic fracture surface remains perpendicular to the axis of the shaft, irrespective of the ratio of K_I/K_{III}. However, under mode III loading, the fracture surface becomes very rough. The roughness greatly exceeds the crack opening displacements and it is clear that the microscopic crack path deviates appreciably from a planar configuration. Due to the abrasion between the crack faces, it is usually difficult to discern any pattern in the path followed by the crack. An elegant experiment which avoided this difficulty has been described by Sommer (1969). The experiment involved fracturing circumferentially notched glass tubes under combined internal pressure and torsion. The pressurized fluid penetrated the crack and alleviated the effects of crack face friction. Under these conditions, several striking features of the crack path were revealed. It appeared that if the ratio of K_{III}/K_I were below a critical value, the crack remained in its initial plane and produced a smooth fracture surface. However, if the loading was such that this ratio was exceeded, then the crack adopted a wavy configuration. A characteristic pattern was observed in the roughness of the crack faces. Initially, the roughness had a small wavelength and amplitude, but as the crack continued to propagate, both the wavelength and amplitude progressively increased. The slope of the surface roughness was found to increase with crack length.

There have been few theoretical studies of three-dimensional non-planar crack growth. The main difficulty is that, in order to predict the crack path, it is necessary to calculate stress intensity factors for cracks with a complicated three-dimensional geometry. Numerical solutions can be costly and sophisticated adaptive meshing schemes are required in order to model incremental crack growth. There have been some attempts to extend Cotterell and Rice's perturbation method to three-dimensional cracks. For example, Faber and Evans (1983) assumed that if a crack is deflected slightly from a planar configuration, the stress intensity factors on the deflected crack front may be found by expressing the asymptotic crack tip fields as components relative to axes oriented with the perturbed crack tip. They used their estimates to determine the toughening caused by second phase particles in a solid, which tend to deflect cracks that run into them. Another method of analysis has been developed by Gao (1992). Using a perturbation expansion of the stress field around a planar crack, he attempted to reduce the non-planar crack problem to an equivalent one involving a planar crack subjected to non-uniform crack face tractions. He used his results to investigate the stability of an initially planar semi-infinite crack under mixed mode loading.

The objective of this paper is to develop a three-dimensional model of non-planar crack growth under mixed mode loading. We begin by describing a perturbation scheme, which can be used to estimate stress intensity factors for slightly wavy cracks in an isotropic, linear elastic solid. The method is a three-dimensional analogue of the perturbation scheme developed by Cotterell and Rice (1980). The spirit of our analysis is similar to Gao's (1992) model, but we have used a different method of solution. While Gao's method is based on a perturbation expansion of the stress field about a planar crack, we have chosen to perturb the integral equation for the displacement jump across the crack faces. Both solutions reduce the wavy crack problem to an equivalent one involving a planar crack loaded by

prescribed tractions on its faces. The two methods lead to different results and the discrepancy between them is discussed further in Appendix A. The accuracy of our perturbation method has been investigated by comparing the results to full-field numerical calculations.

We have used the perturbation solution to investigate the path followed by an initially planar semi-infinite crack, which is subjected to remote loading. In particular, we have attempted to determine the conditions where the crack may deviate from its initial plane and propagate in a wavy fashion. For the case of mixed mode I/mode II loading, we recover the results of Cotterell and Rice (1980). For mixed mode I/mode III loading, we have found that the crack tends to deviate from its initial plane if the ratio of K_{III}/K_I exceeds a critical value, which depends on Poisson's ratio. The role of T-stresses which act parallel to the plane of the planar crack has also been investigated.

Finally, we present some three-dimensional numerical simulations of crack growth under mixed mode loading. Our solutions were obtained using a boundary integral formulation developed by Xu and Ortiz (1993). The results confirm the stability criteria predicted by the perturbation analysis. In the cases where the crack propagates along a wavy path, we have found remarkably good agreement between the numerical results and experimental observations reported in the literature.

2. PERTURBATION SOLUTION TO NON-PLANAR CRACK PROBLEMS

We begin by describing a method for calculating stress intensity factors at the tip of a slightly wavy three-dimensional crack. Figure 1 illustrates the problem to be solved. Consider an isotropic, linear elastic solid with shear modulus μ and Poisson's ratio ν. Suppose that the material contains a crack, which lies on an arbitrary non-planar surface S and is bounded by a smooth curve C. The solid is loaded by a distribution of remote loads and we wish to determine the resulting distribution of stress intensity factors $K_I(s)$, $K_{II}(s)$ and $K_{III}(s)$ on C. In general, this problem is too difficult to solve without recourse to a numerical method. We therefore simplify the analysis by reducing the non-planar crack problem to an equivalent one involving a planar reference crack subjected to non-uniform crack face tractions.

It is well known that a crack in an elastic solid may be represented by a distribution of dislocations. The distribution is chosen so as to produce the correct displacement jump across the surface S. Thus, suppose that the stress induced at a point $\mathbf{x}$ in the uncracked solid by the remote loading is $\boldsymbol{\sigma}^\infty(\mathbf{x})$. Imagine that the relative displacement of the crack faces at a point $\boldsymbol{\xi}$ on S is known to be $\mathbf{u}(\boldsymbol{\xi})$. Then, the stress at $\mathbf{x}$ in the cracked solid may be expressed as

$$\boldsymbol{\sigma}(\mathbf{x}) = \boldsymbol{\sigma}^\infty(\mathbf{x}) + \int_S \mathbf{F}(\boldsymbol{\xi}, \mathbf{x}) \nabla \mathbf{u}(\boldsymbol{\xi}) \, \mathrm{d}A_\xi, \tag{1}$$

where ∇ is the gradient operator. Full expressions for $\mathbf{F}$ will be given later. Conveniently, it is found that $\mathbf{F}$ depends only on the distance between $\mathbf{x}$ and $\boldsymbol{\xi}$ and on the normal to S at $\boldsymbol{\xi}$, and is otherwise independent of the geometry of the crack. In particular, it does not depend on the curve C which bounds the cracked surface. In general, the crack face

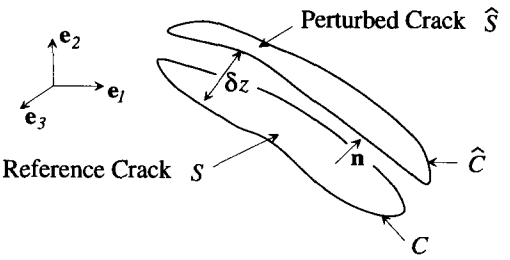

Fig. 1. A crack with a reference geometry for which stress intensity factors and weight functions are known, perturbed to a new geometry.

displacements are not known *a priori*, and eqn (1) is used to formulate an integral equation to be solved for $\mathbf{u}(\xi)$. Since the faces of the crack are free of tractions, we have that

$$\int_S [\mathbf{F}(\xi, \mathbf{x})\nabla\mathbf{u}(\xi)]\mathbf{n}(\mathbf{x})\,\mathrm{d}A_\xi + \mathbf{t}(\mathbf{x}) = 0 \quad [\mathbf{x} \in S], \tag{2}$$

where $\mathbf{n}(\mathbf{x})$ is the unit normal to the crack surface at $\mathbf{x}$, and $\mathbf{t} = \boldsymbol{\sigma}^\infty(\mathbf{x})\mathbf{n}(\mathbf{x})$. Here, $\mathbf{t}$ plays the role of a distribution of tractions acting on the crack faces, which induce the crack opening displacements $\mathbf{u}$. Equation (2) is often used as the basis of a boundary integral method for solving three-dimensional crack problems (Fares, 1989; Xu and Ortiz, 1993).

For a few crack geometries, the integral eqn (2) may be inverted explicitly. In this case, we may write

$$\mathbf{u}(\mathbf{x}) = \int_S \mathbf{G}(\mathbf{x}, \xi)\mathbf{t}(\xi)\,\mathrm{d}A. \tag{3}$$

In eqn (3), $\mathbf{G}(\mathbf{x}, \xi)$ represents the relative crack face displacements at $\mathbf{x}$ due to a pair of unit point loads acting at a point ξ on the crack faces. The stress intensity factors may then be deduced from the asymptotic variation of the crack face displacements $\mathbf{u}(\mathbf{x})$ as $\mathbf{x}$ approaches the crack front C. The result may be expressed in the following form

$$K_\alpha(s) = \int_S \mathbf{h}^\alpha(\mathbf{x}, s) \cdot \mathbf{t}(\mathbf{x})\,\mathrm{d}A, \tag{4}$$

where K_α is an abbreviation for the three possible stress intensity factors K_I, K_II and K_III. In eqn (4), $\mathbf{h}^\alpha(\mathbf{x}, s)$ is the crack face weight function for the solid and represents the stress intensity factors at a point s on C due to a pair of point loads acting at $\mathbf{x}$ on S.

Provided that the weight function $\mathbf{h}^\alpha$ is known, stress intensity factors for the crack may be deduced by first calculating the distribution of stress $\boldsymbol{\sigma}^\infty$ in the uncracked solid, and then evaluating the integral in eqn (4). The limitation of this method is that closed form expressions for $\mathbf{h}^\alpha$ are known for only two three-dimensional crack geometries. These are a planar circular crack and a planar semi-infinite crack. However, we will show that these results may be used to estimate stress intensity factors for cracks which have a geometry that is close to that of a penny shaped crack, or a planar semi-infinite crack.

Consider the following issue: suppose that there exists a crack with a particular geometry, characterized by a surface S and a bounding curve C for which $\mathbf{F}$, $\mathbf{G}$ and $\mathbf{h}^\alpha$ are known. Following the procedure outlined above, we may calculate the crack face displacements $\mathbf{u}(\mathbf{x})$ and stress intensity factors K_α for this crack geometry. Now, imagine that the crack is perturbed slightly from its original configuration (Fig. 1). We choose a mapping such that $\mathbf{x} \to \hat{\mathbf{x}}$, where

$$\hat{\mathbf{x}} = \mathbf{x} + \delta z(\mathbf{x})\mathbf{n}(\mathbf{x}), \quad \hat{\xi} = \xi + \delta z(\xi)\mathbf{n}(\xi). \tag{5}$$

Here, $\mathbf{n}$ is a unit vector perpendicular to the original crack, and $\delta z_{,i} \ll 1$. As a result, the opening displacements and stress intensity factors on the perturbed crack become

$$\begin{aligned} \hat{\mathbf{u}} &= \mathbf{u} + \delta\mathbf{u}, \\ \hat{K}_\alpha &= K_\alpha + \delta K_\alpha. \end{aligned} \tag{6}$$

Our objective is to calculate $\delta\mathbf{u}$ and δK_α to first-order in δz.

To this end, we formulate the integral eqn (2) for the perturbed geometry

$$\int_S [\mathbf{F}(\hat{\boldsymbol{\xi}}, \hat{\mathbf{x}}) \nabla \hat{\mathbf{u}}(\hat{\boldsymbol{\xi}})] \hat{\mathbf{n}}(\hat{\mathbf{x}}) \, dA_{\xi} + \hat{\mathbf{t}}(\hat{\mathbf{x}}) = 0 \quad [\hat{\mathbf{x}} \in \hat{S}], \tag{7}$$

where $\hat{\mathbf{n}}(\hat{\mathbf{x}}) = \mathbf{n}(\mathbf{x}) + \delta\mathbf{n}(\mathbf{x})$ is the normal to the perturbed crack at $\hat{\mathbf{x}}$, and $\hat{\mathbf{t}} = \boldsymbol{\sigma}^{\infty}(\hat{\mathbf{x}})\hat{\mathbf{n}}(\hat{\mathbf{x}})$. Now, expanding to first order in each perturbed variable, eqn (7) may be approximated by

$$\int_S [(\mathbf{F}(\boldsymbol{\xi}, \mathbf{x}) + \delta\mathbf{F}(\boldsymbol{\xi}, \mathbf{x})) \nabla(\mathbf{u} + \delta\mathbf{u})](\mathbf{n} + \delta\mathbf{n}) \, dA_{\xi} + [\mathbf{t} + \delta\mathbf{t}] = 0, \tag{8}$$

where $\delta\mathbf{t} = [\nabla\boldsymbol{\sigma}^{\infty}\delta\mathbf{x}]\mathbf{n}(\mathbf{x}) + \boldsymbol{\sigma}^{\infty}\delta\mathbf{n}(\mathbf{x})$ and $\delta\mathbf{F}$ is an abbreviation for

$$\delta\mathbf{F}(\mathbf{x}, \boldsymbol{\xi}) = \frac{\partial \mathbf{F}(\boldsymbol{\xi}, \mathbf{x})}{\partial \boldsymbol{\xi}} \delta\boldsymbol{\xi} + \frac{\partial \mathbf{F}(\boldsymbol{\xi}, \mathbf{x})}{\partial \mathbf{x}} \delta\mathbf{x}, \tag{9}$$

with $\delta\mathbf{x} = \delta z(\mathbf{x})\mathbf{n}(\mathbf{x})$, $\delta\boldsymbol{\xi} = \delta z(\boldsymbol{\xi})\mathbf{n}(\boldsymbol{\xi})$. Using eqn (2) and discarding second-order terms, we find that eqn (9) may be simplified to

$$\int_S [\mathbf{F}(\boldsymbol{\xi}, \mathbf{x}) \nabla \delta\mathbf{u}(\boldsymbol{\xi})]\mathbf{n}(\mathbf{x}) \, dA_{\xi} + \mathbf{t}^{\text{eff}}(\mathbf{x}) = 0, \tag{10}$$

where

$$\mathbf{t}^{\text{eff}}(\mathbf{x}) = [\nabla\boldsymbol{\sigma}^{\infty}\delta\mathbf{x}]\mathbf{n}(\mathbf{x}) + \boldsymbol{\sigma}^{\infty}\delta\mathbf{n}(\mathbf{x}) + \int_S [\mathbf{F}(\boldsymbol{\xi}, \mathbf{x}) \nabla \mathbf{u}(\boldsymbol{\xi})] \delta\mathbf{n}(\mathbf{x}) \, dA_{\xi}$$

$$+ \int_S [\delta\mathbf{F}(\boldsymbol{\xi}, \mathbf{x}) \nabla \mathbf{u}(\boldsymbol{\xi})]\mathbf{n}(\mathbf{x}) \, dA_{\xi} + \int_S [\mathbf{F}(\boldsymbol{\xi}, \mathbf{x}) \nabla \mathbf{u}(\boldsymbol{\xi})]\mathbf{n}(\mathbf{x}) [\nabla \cdot (\delta z(\boldsymbol{\xi})\mathbf{n}(\boldsymbol{\xi}))] \, dA_{\xi}. \tag{11}$$

Clearly, eqn (10) is the integral equation for a crack of the unperturbed geometry, which is loaded by crack face tractions $\mathbf{t}^{\text{eff}}$. The apparent tractions can be computed for any perturbation of a three-dimensional crack, regardless of its initial geometry. Then, $\delta\mathbf{u}$ and δK_{α} may be computed by replacing $\mathbf{t}$ by $\mathbf{t}^{\text{eff}}$ in eqns (3) and (4). Of course, this procedure can only be applied if the crack face weight functions are available for the initial crack, so that for practical purposes we are limited to considering cracks which are close to penny shaped, or close to a semi-infinite crack.

The integrals in eqn (11) must be evaluated with care. Although the tractions $\mathbf{t}^{\text{eff}}$ are continuous across the crack faces, the separate integrals which contribute to $\mathbf{t}^{\text{eff}}$ are not. Both the first and second integrals in eqn (11) have different values on the top and bottom crack faces and must be evaluated through a limiting process by letting $\mathbf{x}$ approach the surface S from above or below. It may be shown that the discontinuous terms in the two integrals always cancel one another. An example is given in Appendix B, where the integrals are evaluated for the special case of a planar, semi-infinite crack which is perturbed to a wavy surface.

There is a second minor complication in applying this procedure. By examining specific cases, we have found that the integrals in eqn (11) are undefined unless $\delta z(\boldsymbol{\xi}) \to 0$ and $\nabla\delta z(\boldsymbol{\xi}) \to 0$ as $\boldsymbol{\xi} \to \mathbf{x}(s)$. In other words, the perturbed crack must be tangential to the unperturbed crack at the point s on C where we are calculating $\delta K_{\alpha}(s)$. At first sight, this appears to limit severely the type of perturbations in geometry that we may consider. However, this difficulty can be circumvented by noting that one can always apply a suitable rotation and translation to the original crack in order to set up a reference crack, which is tangential to the perturbed geometry at the appropriate point. It is usually straightforward to find the change in stress intensity factor associated with setting up the reference crack. This procedure is illustrated in Appendix B.

To complete the discussion, we give explicit expressions for the kernel $\mathbf{F}$ in eqn (1), and its perturbation $\delta\mathbf{F}$ in eqn (9). Following the steps outlined in Xu and Ortiz (1993), we find that

$$\int_S \mathbf{F}(\mathbf{x},\boldsymbol{\xi})\nabla\mathbf{u}(\boldsymbol{\xi}) \equiv \frac{\mu}{4\pi}\int_S \left[(\mathbf{e}_i\times\nabla)\frac{1}{R}\right]\otimes(\mathbf{n}(\boldsymbol{\xi})\times\nabla u_i(\boldsymbol{\xi}))\,\mathrm{d}A_\xi + \frac{\mu}{4\pi}\int_S (\mathbf{n}(\boldsymbol{\xi})\times\nabla u_i(\boldsymbol{\xi}))\otimes\left[(\mathbf{e}_i\times\nabla)\frac{1}{R}\right]\mathrm{d}A_\xi - \frac{\mu}{4\pi(1-\nu)}\int_S [\mathbf{e}_i\times(\mathbf{n}(\boldsymbol{\xi})\times\nabla u_i(\boldsymbol{\xi}))][\nabla(\nabla\otimes\nabla-\mathbf{I}\nabla^2)R]\,\mathrm{d}A_\xi, \quad (12)$$

where summation on i is implied. In eqn (12), $\mathbf{n}(\boldsymbol{\xi})$ denotes the normal to S at $\boldsymbol{\xi}$, $\mathbf{I}$ is the identity tensor and $R = |\mathbf{x}-\boldsymbol{\xi}|$. Also, u_i are the Cartesian components of $\mathbf{u}$, and $\mathbf{e}_i$ are the basis vectors. The symbol $\nabla \equiv \mathbf{e}_k\partial/\partial\xi_k$, while $\times$ denotes a vector product and $\otimes$ a dyadic product. Now, to perturb the operator and calculate $\delta\mathbf{F}$, we let $\boldsymbol{\xi}\to\boldsymbol{\xi}+\delta z_\xi\mathbf{n}(\boldsymbol{\xi})$, $\mathbf{x}\to\mathbf{x}+\delta z_x\mathbf{n}(\mathbf{x})$ and $\mathbf{n}\to\mathbf{n}+\delta\mathbf{n}$, and expand each term to first-order, with the result

$$\begin{aligned}\int_S \delta\mathbf{F}(\mathbf{x},\boldsymbol{\xi})\nabla\mathbf{u}(\boldsymbol{\xi})\,\mathrm{d}A_\xi \equiv{}& \frac{\mu}{4\pi}\int_S\left[\mathbf{e}_i\times\left(\delta z_\xi\frac{\partial}{\partial\mathbf{n}_\xi}+\delta z_x\frac{\partial}{\partial\mathbf{n}_x}\right)\nabla R^{-1}\right]\otimes(\mathbf{n}(\boldsymbol{\xi})\times\nabla u_i(\boldsymbol{\xi}))\,\mathrm{d}A_\xi\\ &+\frac{\mu}{4\pi}\int_S(\mathbf{n}(\boldsymbol{\xi})\times\nabla u_i(\boldsymbol{\xi}))\otimes\left[\mathbf{e}_i\times\left(\delta z_\xi\frac{\partial}{\partial\mathbf{n}_\xi}+\delta z_x\frac{\partial}{\partial\mathbf{n}_x}\right)\nabla R^{-1}\right]\mathrm{d}A_\xi\\ &+\frac{\mu}{4\pi}\int_S(\mathbf{e}_i\times\nabla R^{-1})\otimes(\delta\mathbf{n}\times\nabla u_i(\boldsymbol{\xi}))\,\mathrm{d}A_\xi+\frac{\mu}{4\pi}\int_S(\delta\mathbf{n}\times\nabla u_i(\boldsymbol{\xi}))\otimes(\mathbf{e}_i\times\nabla R^{-1})\,\mathrm{d}A_\xi\\ &-\frac{\mu}{4\pi(1-\nu)}\int_S[\mathbf{e}_i\times(\delta\mathbf{n}\times\nabla u_i(\boldsymbol{\xi}))][\nabla(\nabla\otimes\nabla-\mathbf{I}\nabla^2)R]\,\mathrm{d}A_\xi\\ &-\frac{\mu}{4\pi(1-\nu)}\int_S[\mathbf{e}_i\times(\mathbf{n}\times\nabla u_i(\boldsymbol{\xi}))]\left[\left(\delta z_\xi\frac{\partial}{\partial\mathbf{n}_\xi}+\delta z_x\frac{\partial}{\partial\mathbf{n}_x}\right)\nabla(\nabla\otimes\nabla-\mathbf{I}\nabla^2)R\right]\mathrm{d}A_\xi \quad (13)\end{aligned}$$

where $\partial R/\partial\mathbf{n}_\xi \equiv [\partial R/\partial\boldsymbol{\xi}]\cdot\mathbf{n}(\boldsymbol{\xi})$ and $\partial R/\partial\mathbf{n}_x \equiv [\partial R/\partial\mathbf{x}]\cdot\mathbf{n}(\mathbf{x})$.

3. PERTURBATION OF A PLANAR SEMI-INFINITE CRACK WITH A STRAIGHT FRONT

We proceed to apply the perturbation method to calculate stress intensity factors for a slightly wavy semi-infinite crack. For this case, the original crack geometry is taken to be a planar, semi-infinite crack which lies on the (x_2, x_3) plane (Fig. 2). Clearly, this choice of reference geometry has one limitation: the projection of the perturbed crack front on the (x_2, x_3) plane is always straight. This restriction is relaxed in the next section by applying a second perturbation to the reference crack, but we will ignore this difficulty for now. The solid is loaded by a uniform distribution of stress $\boldsymbol{\sigma}^\infty$ at infinity. The stress components

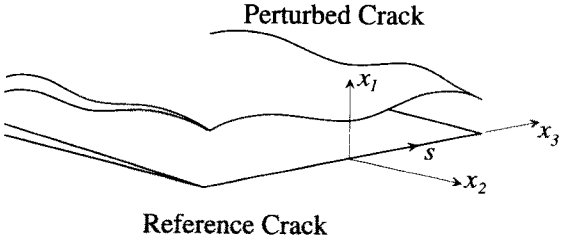

Fig. 2. Perturbation of a planar semi-infinite crack into a non-planar configuration.

σ_{11}^{∞}, σ_{12}^{∞} and σ_{13}^{∞} are such that uniform stress intensity factors K_{I}, K_{II} and K_{III} are induced on the planar crack. The corresponding crack opening displacements $\mathbf{u}$ are

$$u_1 = K_{\mathrm{I}}^{\infty}\frac{4(1-\nu)}{\mu}\sqrt{\frac{-x_2}{2\pi}}, \quad u_2 = K_{\mathrm{II}}^{\infty}\frac{4(1-\nu)}{\mu}\sqrt{\frac{-x_2}{2\pi}}, \quad u_3 = K_{\mathrm{III}}^{\infty}\frac{4}{\mu}\sqrt{\frac{-x_2}{2\pi}}. \tag{14}$$

In addition, the solid may be subjected to so called T-stresses, which act parallel to the planar crack and so do not induce stress intensity factors, but which induce non-zero stress intensity factors on the perturbed crack. We will denote the T-stress components by

$$\sigma_{22}^{\infty} = T_{22}, \quad \sigma_{33}^{\infty} = T_{33} + \nu\sigma_{11}^{\infty}, \quad \sigma_{23}^{\infty} = T_{23}. \tag{15}$$

The second of eqn (15) has been written so that if $T_{ij} = 0$, the solid deforms in a state of plane strain.

Now, suppose that the crack is perturbed slightly from its planar configuration, so that a point at $(0, x_2, x_3)$ on the cracked surface is displaced to $(\delta z, x_2, x_3)$, with $\delta z_{,i} \ll 1$. The perturbation in geometry must also vanish far from the crack front; $\delta z \to 0$ as $x_2 \to -\infty$. We seek to calculate the change in stress intensity factors $\delta K_{\alpha}(s)$ at a point s on the crack front due to this perturbation. To do so, we apply the procedure outlined in the preceding section.

Evaluating the integrals in eqn (11) for a semi-infinite crack poses some difficulties, due to the ambiguous nature of the remote loading. The simplest way to avoid this difficulty is to represent the semi-infinite crack by a bounded slit crack of width c, so that the crack lies in the region $\{x_1 = 0, -c \leqslant x_2 \leqslant 0, -\infty \leqslant x_3 \leqslant \infty\}$. The slit crack is assumed to be perturbed near one tip. One may then calculate the effective tractions in eqn (11) without difficulty, and the change in stress intensity factors on the perturbed crack front follow. Finally, to obtain results for a semi-infinite crack, we let the size of the slit crack $c \to \infty$. The details involved in this procedure are somewhat lengthy and are described fully in Appendix B.

It is shown that two effects contribute to the change in stress intensity factors on the perturbed crack front. First, one must rotate and translate the planar crack to a reference configuration, which is tangential to the perturbed crack at the point s. This ensures that the integrals in eqn (11) are regular. The reference crack is then subjected to a second perturbation so that it reaches the wavy configuration. In Appendix B, it is shown that the change in stress intensity factors due to the regularization process is

$$\begin{aligned}
\delta K_{\mathrm{I}}^{\mathrm{reg}} &= -\delta z[\mathbf{x}(s)]_{,2}K_{\mathrm{II}}^{\infty} - \frac{1}{1-\nu}\delta z[\mathbf{x}(s)]_{,3}K_{\mathrm{III}}^{\infty},\\
\delta K_{\mathrm{II}}^{\mathrm{reg}} &= \delta z[\mathbf{x}(s)]_{,2}K_{\mathrm{I}}^{\infty},\\
\delta K_{\mathrm{III}}^{\mathrm{reg}} &= (1-\nu)\delta z[\mathbf{x}(s)]_{,3}K_{\mathrm{I}}^{\infty},
\end{aligned} \tag{16}$$

accurate to first-order in δz. The remaining contribution to δK_{α} arises when the crack is perturbed from the reference configuration to the final wavy surface. It may be calculated using the following procedure. First, one finds a distribution of effective tractions t_i^{eff} that act on a planar semi-infinite crack. In Appendix B, we show that the tractions are given by

$$t_i^{\mathrm{eff}}(\mathbf{x}) = \frac{K_{\mathrm{I}}^{\infty}}{(2\pi)^{3/2}}\,\mathrm{PV}\int_S \frac{1}{R^3\sqrt{-\xi_2}}\left\{[\delta z(\boldsymbol{\xi}) - \delta z(\mathbf{x})]\left(\delta_{i2} - \frac{3r_2(\delta_{i2}r_2 + \delta_{i3}r_3)}{R^2}\right)\right.$$

$$\left. -(1-\nu)\delta z_{,3}(\boldsymbol{\xi})(r_2\delta_{i3} - r_3\delta_{i2})\right\}\mathrm{d}A_{\xi}$$

$$-\frac{K_{II}^{\infty}}{(2\pi)^{3/2}}\,\mathrm{PV}\int_S \frac{\delta_{i1}}{R^3\sqrt{-\xi_2}}\{\delta z(\xi)-\delta z(\mathbf{x})+(1-2\nu)r_3\delta z_{,3}(\xi)\}\,\mathrm{d}A_\xi$$

$$+\frac{K_{III}^{\infty}}{(2\pi)^{3/2}}\frac{(1-2\nu)}{(1-\nu)}\,\mathrm{PV}\int_S \frac{\delta_{i1}r_2\delta z_{,3}(\xi)}{R^3\sqrt{-\xi_2}}\,\mathrm{d}A_\xi - T_{i2}\delta z_{,2}(\mathbf{x})-T_{i3}\delta z_{,3}(\mathbf{x}), \tag{17}$$

where δ_{ij} denotes the Kronecker delta and

$$r_i = x_i-\xi_i, \quad R=\sqrt{r_i r_i}. \tag{18}$$

The symbol PV as been used to show that Cauchy Principle Values should be taken for the integrals.

The stress intensity factors induced by these tractions follow from eqn (4) as

$$\delta K_\alpha^p(s) = \int_S h_i^\alpha(\mathbf{x},s)t_i^{\mathrm{eff}}(\mathbf{x})\,\mathrm{d}A_x. \tag{19}$$

The weight functions for a semi-infinite crack may be found in several references (Ulfyand, 1965; Kassir and Sih, 1973; Bueckner, 1970) and are given by

$$h_1^{\mathrm{I}} = \sqrt{\frac{2}{\pi^3}}\frac{\sqrt{-x_2}}{[x_2^2+(x_3-s)^2]},\quad h_2^{\mathrm{I}} = h_3^{\mathrm{I}} = 0,$$

$$h_2^{\mathrm{II}} = \sqrt{\frac{2}{\pi^3}}\frac{\sqrt{-x_2}}{[x_2^2+(x_3-s)^2]}\left(1+\frac{2\nu}{(2-\nu)}\frac{[x_2^2-(x_3-s)^2]}{[x_2^2+(x_3-s)^2]}\right),$$

$$h_3^{\mathrm{III}} = \sqrt{\frac{2}{\pi^3}}\frac{\sqrt{-x_2}}{[x_2^2+(x_3-s)^2]}\left(1-\frac{2\nu}{(2-\nu)}\frac{[x_2^2-(x_3-s)^2]}{[x_2^2+(x_3-s)^2]}\right),$$

$$h_3^{\mathrm{II}} = h_2^{\mathrm{III}} = \sqrt{\frac{2}{\pi^3}}\frac{\sqrt{-x_2}}{[x_2^2+(x_3-s)^2]}\left(\frac{-4\nu}{(2-\nu)}\frac{x_2(x_3-s)}{[x_2^2+(x_3-s)^2]}\right),$$

$$h_1^{\mathrm{II}} = h_1^{\mathrm{III}} = 0. \tag{20}$$

Finally, the stress intensity factors on the perturbed semi-infinite crack are given by the sum of eqns (16) and (19)

$$\begin{aligned} K_{\mathrm{I}}(s) &= K_{\mathrm{I}}^{\infty}+\delta K_{\mathrm{I}}^{\mathrm{reg}}+\delta K_{\mathrm{I}}^{p}(s),\\ K_{\mathrm{II}}(s) &= K_{\mathrm{II}}^{\infty}+\delta K_{\mathrm{II}}^{\mathrm{reg}}+\delta K_{\mathrm{II}}^{p}(s),\\ K_{\mathrm{III}}(s) &= K_{\mathrm{III}}^{\infty}+\delta K_{\mathrm{III}}^{\mathrm{reg}}+\delta K_{\mathrm{III}}^{p}(s). \end{aligned} \tag{21}$$

As an example, consider a two-dimensional perturbation of the form

$$\delta z(x_2) = \begin{cases}\lambda(x_2) & x_2 \geqslant -a,\\ 0 & x_2 \leqslant -a.\end{cases} \tag{22}$$

For this case, the changes in K_α due to regularizing the integrals are

$$\begin{aligned} \delta K_{\mathrm{I}}^{\mathrm{reg}} &= -\lambda'(0)K_{\mathrm{II}}^{\infty},\\ \delta K_{\mathrm{II}}^{\mathrm{reg}} &= \lambda'(0)K_{\mathrm{I}}^{\infty}, \end{aligned}$$

$$\delta K_{\mathrm{III}}^{\mathrm{reg}} = 0, \tag{23}$$

where $\lambda' \equiv \mathrm{d}\lambda/\mathrm{d}x_2$. The effective tractions in eqn (17) may be reduced to

$$\begin{aligned}
t_1^{\mathrm{eff}}(x_2) &= \frac{-2K_{\mathrm{II}}^{\infty}}{(2\pi)^{3/2}}\,\mathrm{PV}\int_{-\infty}^{0}\frac{\delta z(\xi)-\delta z(x_2)}{(\xi-x_2)^2\sqrt{-\xi}}\,\mathrm{d}\xi,\\
t_2^{\mathrm{eff}}(x_2) &= \frac{-2K_{\mathrm{I}}^{\infty}}{(2\pi)^{3/2}}\,\mathrm{PV}\int_{-\infty}^{0}\frac{\delta z(\xi)-\delta z(x_2)}{(\xi-x_2)^2\sqrt{-\xi}}\,\mathrm{d}\xi - T_{22}\lambda'(x_2),\\
t_3^{\mathrm{eff}}(x_2) &= -T_{32}\lambda'(x_2).
\end{aligned} \tag{24}$$

Finally, the change in stress intensity factors due to perturbing the reference crack are found to be

$$\begin{aligned}
\delta K_{\mathrm{I}}^{p} &= \frac{-K_{\mathrm{II}}^{\infty}}{\pi^2}\lim_{\beta\to 0}\int_{-a+\beta}^{-\beta}\mathrm{d}x\,\mathrm{PV}\int_{-a}^{0}\frac{\lambda(\xi)-\lambda(x)}{(\xi-x)^2\sqrt{\xi x}}\,\mathrm{d}\xi,\\
\delta K_{\mathrm{II}}^{p} &= \frac{-K_{\mathrm{I}}^{\infty}}{\pi^2}\lim_{\beta\to 0}\int_{-a+\beta}^{-\beta}\mathrm{d}x\,\mathrm{PV}\int_{-a}^{0}\frac{\lambda(\xi)-\lambda(x)}{(\xi-x)^2\sqrt{\xi x}}\,\mathrm{d}\xi - T_{22}\sqrt{\frac{2}{\pi}}\int_{-a}^{0}\frac{\lambda'(x)}{\sqrt{-x}}\,\mathrm{d}x,\\
\delta K_{\mathrm{III}}^{p} &= -T_{32}\sqrt{\frac{2}{\pi}}\int_{-a}^{0}\frac{\lambda'(x)}{\sqrt{-x}}\,\mathrm{d}x.
\end{aligned} \tag{25}$$

The first two integrals in eqn (25) may be evaluated by expanding $\lambda(x)$ and $\lambda(\xi)$ in Taylor series about $\xi = x = 0$. The only non-zero term in the resulting series is $\pi^2\lambda'(0)/2$. Combining eqns (23) and (25) then gives the stress intensity factors on the perturbed crack

$$\begin{aligned}
K_{\mathrm{I}} &= K_{\mathrm{I}}^{\infty} - \tfrac{3}{2}\lambda'(0),\\
K_{\mathrm{II}} &= K_{\mathrm{II}}^{\infty} + \tfrac{1}{2}\lambda'(0) - T_{22}\sqrt{\frac{2}{\pi}}\int_{-a}^{0}\frac{\lambda'(x)}{\sqrt{-x}}\,\mathrm{d}x,\\
K_{\mathrm{III}} &= K_{\mathrm{III}}^{\infty} - T_{32}\sqrt{\frac{2}{\pi}}\int_{-a}^{0}\frac{\lambda'(x)}{\sqrt{-x}}\,\mathrm{d}x
\end{aligned} \tag{26}$$

accurate to first order in λ. The same results were found by Cotterell and Rice (1980) by solving the two dimensional problem directly.

The analogous case of a crack which is wavy in the x_3 direction may also be solved exactly. To this end, consider a perturbation of the form $\delta z = A\sin kx_3$. Omitting details of the calculation, the resulting stress intensity factors are found to be

$$\begin{aligned}
K_{\mathrm{I}}(s) &= K_{\mathrm{I}}^{\infty} - K_{\mathrm{II}}^{\infty}Ak\left\{\frac{1}{2}-\frac{(1-2\nu)}{\sqrt{2}}\right\}\sin ks - K_{\mathrm{III}}^{\infty}Ak\left\{2-\frac{(1-2\nu)}{\sqrt{2}(1-\nu)}\right\}\cos ks,\\
K_{\mathrm{II}}(s) &= K_{\mathrm{II}}^{\infty} + K_{\mathrm{I}}^{\infty}Ak\,\frac{1}{2}\left\{1-\frac{2\nu}{(2-\nu)}+\frac{1}{\sqrt{2}}\,\frac{\nu^2}{(2-\nu)}\right\}\sin ks - \frac{A\sqrt{2k}}{2-\nu}(\nu T_{33}\sin ks + 2T_{23}\cos ks),\\
K_{\mathrm{III}}(s) &= K_{\mathrm{III}}^{\infty} + K_{\mathrm{I}}^{\infty}Ak\left\{1+\nu\left(\frac{1}{\sqrt{2}}-2\right)+\frac{\nu}{(2-\nu)}\left(\sqrt{2}-1-\frac{\nu}{2\sqrt{2}}\right)\right\}\cos ks\\
&\quad - \frac{A\sqrt{2k}}{2-\nu}(2(1-\nu)T_{33}\cos ks - \nu T_{23}\sin ks).
\end{aligned} \tag{27}$$

The effects of a more general perturbation of the form $\delta z = \lambda(x_3)$ may be found by taking a sine transform of δz, using eqn (27) to find the sine transform of δK, and inverting the result. Similar results were reported by Gao [1993; eqn (38)], but our expressions contain some additional terms. The cause of this discrepancy is discussed further in Appendix A.

As a final example, which will be useful in the analysis to follow, consider a perturbation of the form

$$\delta z(x_2, x_3) = \begin{cases} (a+x_2)(\gamma+\omega \sin kx_3) & x_2 > -a, \\ 0 & x_2 \leqslant -a. \end{cases} \tag{28}$$

The shape of the crack which corresponds to this perturbation is illustrated in Fig. 3. It consists of a planar semi-infinite crack with a wavy kink at its tip. Following the steps outlined above, we find that the stress intensity factors on the perturbed crack tip are

$$\begin{aligned} K_{\mathrm{I}}(s) &= K_{\mathrm{I}}^{\infty} - \frac{3\gamma}{2} K_{\mathrm{II}}^{\infty} + K_{\mathrm{II}}^{\infty} J_{12}(\nu, ak)\omega \sin ks - K_{\mathrm{III}}^{\infty} J_{13}(\nu, ak)\omega \cos ks, \\ K_{\mathrm{II}}(s) &= K_{\mathrm{II}}^{\infty} + \frac{\gamma}{2} K_{\mathrm{I}}^{\infty} + K_{\mathrm{I}}^{\infty} J_{21}(\nu, ak)\omega \sin ks \\ &\quad - 2\gamma T_{22}\sqrt{\frac{2a}{\pi}} - \sqrt{2/k}[T_{22}S_{222}(\nu, ak) + T_{33}S_{233}(\nu, ak)]\omega \sin ks \\ &\quad - T_{23}\sqrt{2/k}\, S_{223}(\nu, ak)\omega \cos ks, \\ K_{\mathrm{III}}(s) &= K_{\mathrm{III}}^{\infty} + K_{\mathrm{I}}^{\infty} J_{31}(\nu, ak)\omega \cos ks - \sqrt{2/k}[T_{22}S_{322}(\nu, ak) + T_{33}S_{333}(\nu, ak)]\omega \cos ks \\ &\quad - 2\gamma T_{32}\sqrt{\frac{2a}{\pi}} - T_{23}\sqrt{2/k}\, S_{323}(\nu, ak) \sin ks \end{aligned} \tag{29}$$

where

$$\begin{aligned} J_{12}(\nu, \lambda) &= -\frac{3}{2} + \frac{\lambda}{2} + (1-2\nu)\lambda F_1(\lambda), \\ J_{13}(\nu, \lambda) &= \lambda\left[2 + \frac{(1-2\nu)}{(1-\nu)} F_1(\lambda)\right], \end{aligned}$$

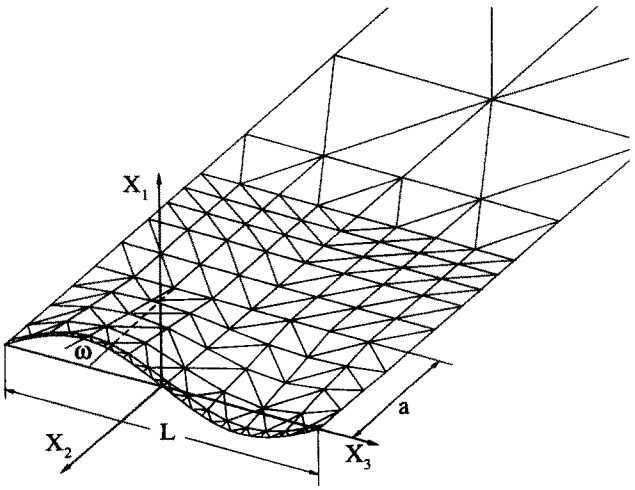

Fig. 3. Semi-infinite crack forming a wavy kink at its tip.

$$J_{21}(v,\lambda)=\frac{1}{2}+\frac{\lambda}{2}\left(1-\frac{2v}{2-v}\right)-\frac{v^2}{2-v}\lambda(F_1(\lambda)-2F_2(\lambda)),$$

$$J_{31}(v,\lambda)=\lambda\left[1-2v-\frac{v}{2-v}-v\left(1+\frac{2}{2-v}\right)F_1(\lambda)+\frac{2v^2}{2-v}F_2(\lambda)\right],$$

$$S_{222}(v,\lambda)=\frac{2}{2-v}\left\{\operatorname{erf}\sqrt{\lambda}-v\sqrt{\frac{\lambda}{\pi}}e^{-\lambda}\right\},$$

$$S_{233}(v,\lambda)=\frac{v}{2-v}\left\{3\sqrt{\frac{\lambda}{\pi}}e^{-\lambda}+\frac{2\lambda-3}{2}\operatorname{erf}\sqrt{\lambda}\right\},$$

$$S_{223}(v,\lambda)=\frac{2}{2-v}\left\{\sqrt{\frac{\lambda}{\pi}}e^{-\lambda}+\frac{2\lambda-1}{2}\operatorname{erf}\sqrt{\lambda}\right\},$$

$$S_{322}(v,\lambda)=\frac{v}{2-v}\left\{\operatorname{erf}\sqrt{\lambda}-2\sqrt{\frac{\lambda}{\pi}}e^{-\lambda}\right\},$$

$$S_{333}(v,\lambda)=\frac{1}{2-v}\left\{2(1-2v)\sqrt{\frac{\lambda}{\pi}}e^{-\lambda}+(2\lambda(1-v)+2v-1)\operatorname{erf}\sqrt{\lambda}\right\},$$

$$S_{323}(v,\lambda)=\frac{1}{2-v}\left\{-v\sqrt{\frac{\lambda}{\pi}}e^{-\lambda}+\frac{4-2v\lambda-v}{2}\operatorname{erf}\sqrt{\lambda}\right\}. \tag{30}$$

In eqn (30), erf denotes the error function and F_1 and F_2 are given by the following expressions;

$$F_1(\lambda)=\frac{\lambda}{\pi^{3/2}}\int_0^\infty\frac{1}{(\lambda^2+s^2)^{1/2}}\operatorname{Re}\left\{\frac{Q(s)}{(\lambda+is)^{1/2}}\right\}ds,$$

$$F_2(\lambda)=\frac{\lambda}{2\pi^{3/2}}\int_0^\infty\frac{1}{(\lambda^2+s^2)^{1/2}}\operatorname{Re}\left\{\frac{\lambda-is}{(\lambda+is)^{3/2}}Q(s)\right\}ds,$$

$$Q(s)=\sqrt{\frac{\pi}{2s}}(1+i)\operatorname{erf}((i-1)\sqrt{s/2})+\frac{i\exp(is)}{s}. \tag{31}$$

For convenience, F_1 and F_2 have been plotted in Fig. 4.

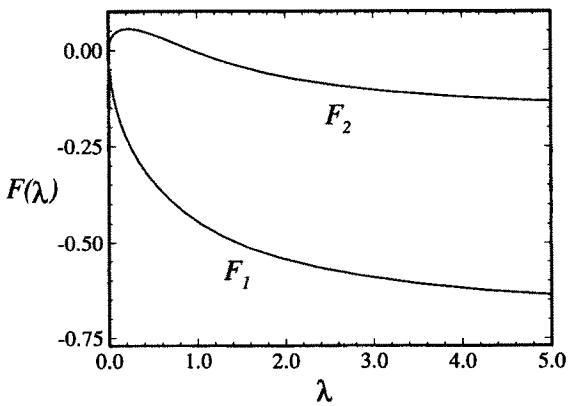

Fig. 4. Dimensionless functions $F_1(\lambda)$ and $F_2(\lambda)$ which appear in the expressions for stress intensity factors for the crack shown in Fig. 3.

4. COMPARISON WITH NUMERICAL SIMULATIONS

The final example given in the preceding section serves as a convenient case to test the range of validity of the results of the first-order perturbation method. With this in mind, we have used a numerical procedure to calculate accurate stress intensity factors for a crack with geometry given in eqn (28). Our numerical scheme is a boundary integral method, which is based on a variational formulation of eqn (2). It is described in detail in Xu and Ortiz (1993) and will only be summarized briefly here.

Xu and Ortiz (1993) show that the potential energy of a cracked solid may be expressed as

$$\Phi[\mathbf{u}] = W[\mathbf{u}] - \int_S \mathbf{t}\cdot\mathbf{u}\,\mathrm{d}S \tag{32}$$

where $\mathbf{u}$ are the crack opening displacements and $\mathbf{t}$ may be thought of as tractions acting on the crack faces as in eqn (2). The term $W[\mathbf{u}]$ represents the elastic strain energy associated with the crack in the solid. It is calculated by representing the crack as a distribution of dislocations. Xu and Ortiz (1993) give the following expression for W;

$$\begin{aligned} W[\mathbf{u}] \equiv \frac{\mu}{4\pi}\int_S\int_S \frac{[\mathbf{e}_i\cdot(\mathbf{n}(\mathbf{x})\times\nabla u_j(\mathbf{x}))][\mathbf{e}_j\cdot(\mathbf{n}(\boldsymbol{\xi})\times\nabla u_j(\boldsymbol{\xi}))]}{R}\,\mathrm{d}A_\xi\,\mathrm{d}A_x \\ -\frac{\mu}{8\pi}\int_S\int_S \frac{[\mathbf{e}_i\cdot(\mathbf{n}(\mathbf{x})\times\nabla u_i(\mathbf{x}))][\mathbf{e}_j\cdot(\mathbf{n}(\boldsymbol{\xi})\times\nabla u_j(\boldsymbol{\xi}))]}{R}\,\mathrm{d}A_\xi\,\mathrm{d}A_x \\ +\frac{\mu}{8\pi(1-\nu)}\int_S\int_S \frac{[\mathbf{e}_i\times(\mathbf{n}(\mathbf{x})\times\nabla u_i(\mathbf{x}))]\mathbf{T}[\mathbf{e}_j\times(\mathbf{n}(\boldsymbol{\xi})\times\nabla u_j(\boldsymbol{\xi}))]}{R}\,\mathrm{d}A_\xi\,\mathrm{d}A_x \end{aligned} \tag{33}$$

where $\mathbf{T}$ is a tensor with components

$$T_{ij} = \frac{\partial R}{\partial x_i\,\partial x_j} \tag{34}$$

and the remaining terms have the same meaning as in eqn (12).

To calculate stress intensity factors for an arbitrarily shaped crack, one must find the distribution of crack opening displacements which minimizes eqn (32). A numerical approximation is found by dividing the surface of the crack into a number of six-noded triangular elements, and using quadratic shape functions to interpolate the crack opening displacements within each element. For elements on the crack front, the mid-side nodes are relocated to quarter-point locations so as to approximate accurately the parabolic variation of opening displacements. By substituting the resulting expressions for the opening displacements into eqn (32), one obtains a system of linear equations for the opening displacements at discrete points on the cracked surface. One advantage of this formulation is that the system of equations is symmetric. Finally, the stress intensity factors are deduced from the asymptotic variation of crack opening displacements near the crack front.

This procedure has been used to calculate stress intensity factors for the crack shown in Fig. 3, for various values of ω and for a value $ak = 2\pi a/L = \pi$. The results are compared with the predictions of the first-order perturbation analysis [eqn (29)] in Fig. 5. In Fig. 5(a), we have plotted the variation of $K_{\mathrm{I}}(s)$, $K_{\mathrm{II}}(s)$ and $K_{\mathrm{III}}(s)$ along the crack front for a crack subjected to remote mode I loading. Results are shown for $ak = \pi$, $\nu = 0.3$, $\gamma = 0$ and various values of ω in eqn (28). It is evident that for small values of ω, the numerical results agree closely with the predictions of the first-order perturbation analysis given in eqn (29). As the angle of the kink increases, so the predictions of the first-order analysis become progressively less accurate. This behavior is illustrated further in Figs 5(b–d), which show the variation in peak values of K_{I}, K_{II} and K_{III} as a function of ω. Results are shown for

three cases: in Fig. 5(b), the crack is subjected to mode I loading; in Fig. 5(c) it is subjected to mode II loading; in Fig. 5(d) results are shown for mode III loading. We conclude that, provided $\omega < 10°$, the first-order results approximate closely to the exact solution.

5. PERTURBATION OF A SEMI-INFINITE CRACK WITH A WAVY FRONT

The solutions to non-planar semi-infinite cracks outlined in Section 3 have one limitation; in each case, the projection of the perturbed crack front on the (x_2, x_3) plane is straight. We proceed to relax this restriction. It is clear that the choice of reference crack determines the shape of the projection of the crack front; to obtain results for more general crack geometries, one must perturb a planar reference crack which has a wavy front. To apply this procedure, solutions are required for the stress intensity factors and the crack face weight functions for the reference crack. While there are no exact solutions for a planar semi-infinite crack with a generally shaped front, approximate solutions have been found by Rice (1985) and Gao and Rice (1986). Their results were obtained using a perturbation method and are accurate provided that the crack front only deviates slightly from a straight line. We will summarize the results of this analysis here, without discussing the derivation. For further details, the reader is referred to Gao and Rice (1986).

The problem to be solved is illustrated in Fig. 6. Suppose that a planar, semi-infinite crack lines in the (x_2, x_3) plane and is loaded by a uniform distribution of remote stress, which induces stress intensity factors K_I^∞, K_{II}^∞, K_{III}^∞ on the crack front. Now, imagine that the crack front is perturbed slightly in the plane of the crack, so that a point at s advances

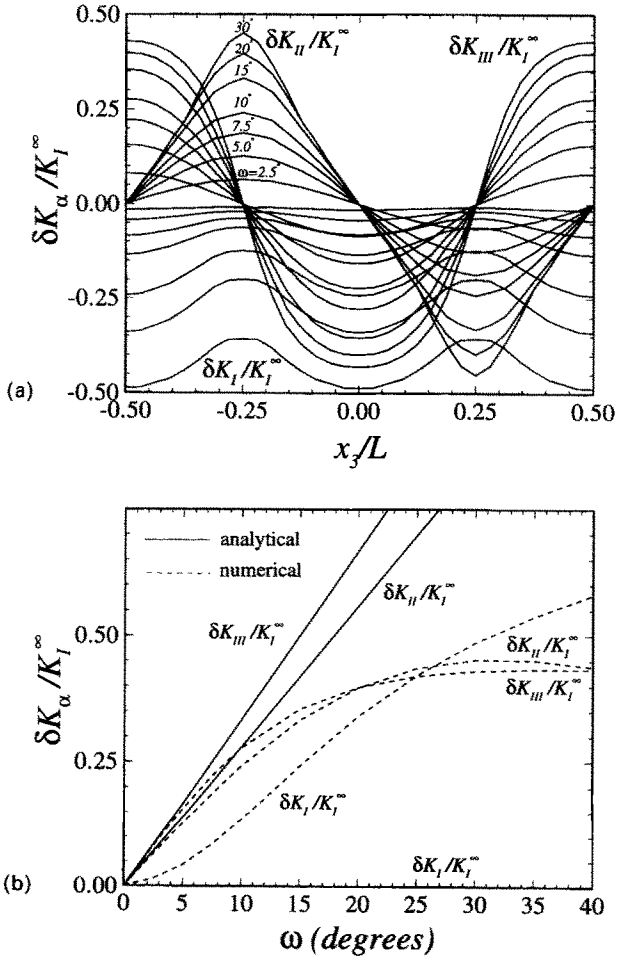

Fig. 5. Comparison of the predictions of the first-order perturbation analysis with accurate numerical simulations. (a) Variation of K along the crack front shown in Fig. 3 for mode I loading; maximum K as a function of kink angle ω for (b) mode I, (c) mode II and (d) mode III remote loading.

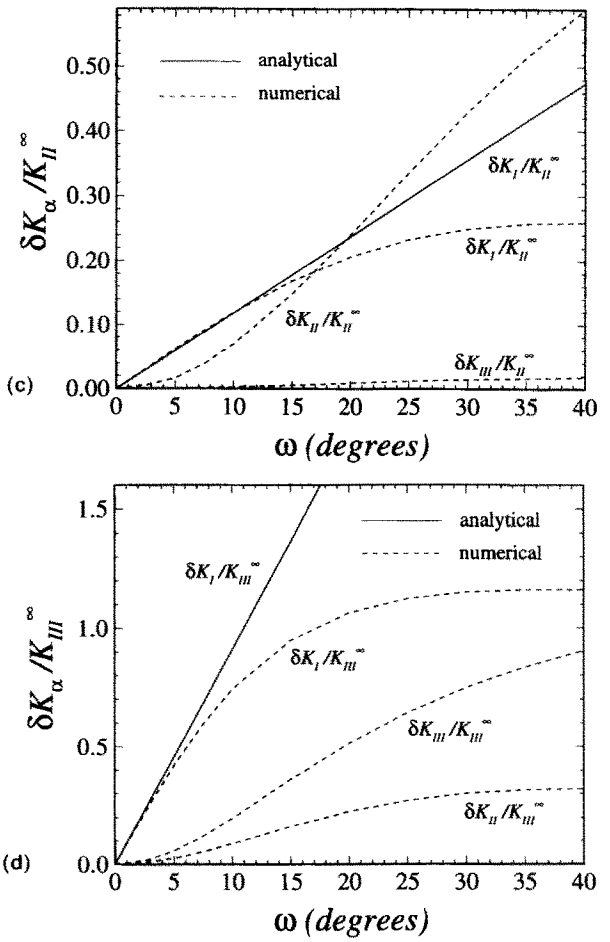

Fig. 5. *Continued.*

a distance $\delta a(s)$. Gao and Rice (1986) show that the stress intensity factors at a point t on the perturbed crack front are given by

$$K_I(t) = K_I^\infty + K_I^\infty F_3(t),$$

$$K_{II}(t) = K_{II}^\infty - \frac{2}{2-\nu} K_{III}^\infty \delta a'(t) + K_{II}^\infty \frac{2-3\nu}{2-\nu} F_3(t),$$

$$K_{III}(t) = K_{III}^\infty + \frac{2(1-\nu)}{2-\nu} K_{II}^\infty \delta a'(t) + K_{III}^\infty \frac{2+\nu}{2-\nu} F_3(t), \tag{35}$$

where $\delta a' \equiv \mathrm{d}\delta a/\mathrm{d}s$ and $F_3(t)$ denotes

$$F_3(t) = \frac{1}{2\pi} \mathrm{PV} \int_{-\infty}^{+\infty} \frac{\delta a(s) - \delta a(t)}{(t-s)^2} \mathrm{d}s. \tag{36}$$

These results are accurate to first-order in $\delta a(s)$. It is also possible to find expressions for

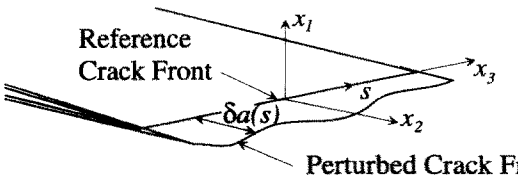

Fig. 6. In-plane perturbation of a semi-infinite crack.

the perturbed crack face weight functions $\mathbf{h}^a$, but we will not require them in the analysis to follow.

As an example, the stress intensity factors for a semi-infinite crack with a cosine-wavy front may be calculated by setting $\delta a(s) = a + B \sin ks + C \cos ks$, which shows that

$$K_I(t) = K_I^\infty\left[1 - \frac{k}{2}(C\cos kt + B\sin kt)\right],$$

$$K_{II}(t) = K_{II}^\infty - K_{II}^\infty \frac{2-3\nu}{2-\nu}\frac{k}{2}(C\cos kt + B\sin kt) - K_{III}^\infty \frac{2}{2-\nu}k(B\cos kt - C\sin kt),$$

$$K_{III}(t) = K_{III}^\infty - K_{III}^\infty \frac{2+\nu}{2-\nu}\frac{k}{2}(C\cos kt + B\sin kt) + K_{II}^\infty \frac{2(1-\nu)}{2-\nu}k(B\cos kt - C\sin kt). \quad (37)$$

Clearly, to generalize the results for a wavy semi-infinite crack given in the preceding section, one may apply two successive perturbations to the crack. The analysis begins by calculating the stress intensity factors for a planar crack with a straight front. The crack is perturbed in its own plane and eqn (35) is used to calculate the resulting change in stress intensity factors. We then perturb the crack a second time, this time in a direction perpendicular to the plane of the original crack. The effects of the second perturbation may be found using the method discussed in the preceding section. Provided that the change in geometry associated with both perturbations is small, one may add the two contributions to the change in crack tip stress intensity factors.

A generalized version of the perturbation in eqn (28) is of particular interest in the stability analysis to follow. Suppose that the semi-infinite crack is first perturbed in its own plane by an amount $\delta a(s) = a + B \sin ks + C \cos ks$, causing the crack front to adopt a wavy configuration. Then an out-of-plane perturbation of the form of eqn (28) is applied to the crack. The resulting configuration of the perturbed crack is similar to the case shown in Fig. 3, except that the projection of the crack front on the (x_2, x_3) plane is sinusoidal. The stress intensity factors on the perturbed crack tip may be expressed in the following form;

$$\begin{aligned}
K_I(s) &= K_I^\infty\left(1 - \frac{k}{2}(C\cos ks + B\sin ks)\right) - \frac{3\gamma}{2}K_{II}^\infty \\
&\quad + K_{II}^\infty J_{12}(\nu, ak)\omega \sin ks - K_{III}^\infty J_{13}(\nu, ak)\omega \cos k, \\
K_{II}(s) &= \frac{\gamma}{2}K_I^\infty + K_I^\infty J_{21}(\nu, ak)\omega \sin ks + K_{II}^\infty\left(1 - \frac{2-3\nu}{2-\nu}\frac{k}{2}(C\cos ks + B\sin ks)\right) \\
&\quad + K_{III}^\infty \frac{2k}{2-\nu}(C\sin ks - B\cos ks) - 2\gamma T_{22}\sqrt{\frac{2a}{\pi}} - [T_{22}S_{222}(\nu, ak) \\
&\quad + T_{33}S_{233}(\nu, ak)]\omega\sqrt{2/k}\sin ks - T_{23}S_{223}(\nu, ak)\omega\sqrt{2/k}\cos ks, \\
K_{III}(s) &= K_I^\infty J_{31}(\nu, ak)\omega \sin ks - K_{II}^\infty \frac{2k(1-\nu)}{2-\nu}(C\sin ks - B\cos ks) \\
&\quad + K_{III}^\infty\left[1 - \frac{2+\nu}{2-\nu}\frac{k}{2}(C\cos ks + B\sin ks)\right] \\
&\quad - 2\gamma T_{32}\sqrt{\frac{2a}{\pi}} - [T_{22}S_{322}(\nu, ak) + T_{33}S_{333}(\nu, ak)]\omega\sqrt{2/k}\cos ks \\
&\quad - T_{23}S_{323}(\nu, ak)\omega\sqrt{2/k}\sin ks. \qquad (38)
\end{aligned}$$

6. STABILITY OF A PLANAR CRACK UNDER MIXED MODE LOADING

The results of our perturbation analysis may be used to investigate the path followed by a semi-infinite crack propagating under remote stress. Suppose that a planar semi-infinite crack is loaded so as to induce uniform stress intensity factors K_{I}^{∞}, K_{II}^{∞}, $K_{\mathrm{III}}^{\infty}$ on its front. The solid may also be subjected to uniform remote T-stresses T_{22}, T_{33}, T_{23}. If the loads reach a critical level, the crack will begin to propagate through the solid. In some circumstances, the crack grows in its initial plane. In others, the crack forms a kink and propagates at an angle to its initial plane. Finally, there are some combinations of remote load which cause the crack to propagate along a wavy path, such that the macroscopic fracture surface remains co-planar with the initial crack, but the crack front deviates from the (x_2, x_3) plane and leaves a rough fracture surface in the wake of the crack. Our objective is to find the conditions necessary for each type of crack growth to occur.

To predict the direction of crack propagation, one must assume an appropriate fracture criterion. It is beyond the scope of this paper to discuss in detail the various criteria for mixed mode fracture which have been proposed in the literature. We have chosen a particular criterion for its simplicity, and it suffices to note that the analysis may be repeated for other fracture criteria, should it prove necessary. We assume that the crack grows so that the local mode II stress intensity factor vanishes at all points on the advancing crack front. In addition, the energy release rate

$$\mathscr{G} = \frac{1-\nu}{2\mu}\left(K_{\mathrm{I}}^2 + \frac{1}{1-\nu}K_{\mathrm{III}}^2\right) \tag{39}$$

must be uniform (and equal to the fracture toughness of the solid) over all propagating regions of the crack.

To investigate the stability of the crack, we look for the conditions where it is possible for a small non-planar kink to form at the crack tip, while satisfying both fracture criteria. To this end, suppose that the crack extends slightly, so that a point at s on the crack front advances a distance $\delta a(s)$, at an angle $\omega(s)$ to the x_2, x_3 plane. For simplicity, we restrict attention to an increment in crack growth such that

$$\delta a(s) = a + B\sin ks + C\cos ks, \quad \omega(s) = \gamma + \omega\sin ks. \tag{40}$$

Recognizing that this crack advance causes the crack to adopt the configuration discussed in the preceding section, we find that the local stress intensity factors on the kink are given by eqn (29). The energy release rate on the perturbed crack may then be computed from eqn (39). We assume that the crack may kink from its initial plane if any combination of B, C, γ, ak and ω can be found such that both $K_{\mathrm{II}} = 0$ and $\mathscr{G}$ is uniform along the crack front.

Consider first the case of a crack subjected to mode I and mode II remote loads, and assume that the T-stresses vanish. Then, the condition $K_{\mathrm{II}} = 0$ requires

$$K_{\mathrm{II}}^{\infty} + \frac{\gamma}{2}K_{\mathrm{I}}^{\infty} = 0, \quad C = 0, \quad K_{\mathrm{I}}^{\infty}J_{21}(\nu, ak)\omega - K_{\mathrm{II}}^{\infty}\frac{2-3\nu}{2-\nu}\frac{Bk}{2} = 0. \tag{41}$$

To first-order, the energy release rate on the advancing crack front is

$$\mathscr{G} = \frac{1-\nu}{2\mu}\left\{(K_{\mathrm{I}}^{\infty})^2 - 3\gamma K_{\mathrm{I}}^{\infty}K_{\mathrm{II}}^{\infty} + 2\left[K_{\mathrm{I}}^{\infty}K_{\mathrm{II}}^{\infty}J_{12}(\nu, ak)\omega - (K_{\mathrm{I}}^{\infty})^2\frac{Bk}{2}\right]\sin ks\right\}. \tag{42}$$

For values of $K_{\mathrm{II}}^{\infty}/K_{\mathrm{I}}^{\infty} < 1.65$ the only solution satisfying both $K_{\mathrm{II}} = 0$ and $\mathscr{G}$ = constant is

$$\gamma = -2K_{II}^{\infty}/K_{I}^{\infty}, \quad \omega = B = 0. \tag{43}$$

This solution corresponds to a kink at the crack tip at an angle γ to the initial crack plane. For values of $K_{II}^{\infty}/K_{I}^{\infty} > 1.65$, it is possible to find non-zero combinations of ω, B and ak which satisfy both fracture criteria. However, our perturbation solution is valid only if $\gamma \ll 1$, so the significance of this result is not clear. We conclude that if a crack is subjected to mode I and mode II loading such that $K_{II}^{\infty}/K_{I}^{\infty} \ll 1$, the crack kinks at an angle γ and is unlikely to develop waviness in a direction parallel to the crack front. This is a well known result and has been derived by a number of authors using various methods of analysis.

Consider next the case of a semi-infinite crack subjected to combined mode I and mode III loading, and again assume that the T-stresses are negligible. In this case, the condition $K_{II} = 0$ shows that

$$\gamma = 0, \quad B = 0, \quad K_{I}^{\infty} J_{21}(\nu, ak)\omega_0 + K_{III}^{\infty} \frac{2Ck}{2-\nu} = 0. \tag{44}$$

Substituting for K_I and K_{III} into the expression for $\mathcal{G}$ in eqn (39), one finds that

$$2\omega K_{III}^{\infty} K_{I}^{\infty}\left(\frac{J_{31}(\nu, ak)}{1-\nu} - J_{13}(\nu, ak)\right) - Ck\left((K_{I}^{\infty})^2 + \frac{2+\nu}{(2-\nu)(1-\nu)}(K_{III}^{\infty})^2\right) = 0 \tag{45}$$

in order to ensure that $\mathcal{G}$ is uniform on the tip of the crack. If

$$\frac{K_{III}^{\infty}}{K_{I}^{\infty}} < 2\sqrt{\frac{2-\nu}{1-\nu}}\left(\frac{(1-\nu)J_{13}(\nu, \lambda \to \infty) - J_{31}(\nu, \lambda \to \infty)}{J_{21}(\nu, \lambda \to \infty)} - \frac{2+\nu}{4}\right)^{-1/2}, \tag{46}$$

then eqns (44) and (45) have only the trivial solution $\omega = C = 0$. For values of $K_{III}^{\infty}/K_{I}^{\infty}$ exceeding this value, non-zero values of ω, C and ak can always be found which satisfy both fracture criteria. We conclude that if $K_{III}^{\infty}/K_{I}^{\infty}$ satisfies the condition (46), then the crack will propagate in its initial plane. Otherwise, the planar configuration is unstable and the crack is likely to propagate along a wavy path. The critical condition for instability is plotted as a function of Poisson's ratio in Fig. 7.

Next, we examine the role of T-stresses in determining the stability of a mode I semi-infinite crack. Suppose first that T_{22} is the only non-zero T-stress component. The condition $K_{II} = 0$ is then satisfied by setting

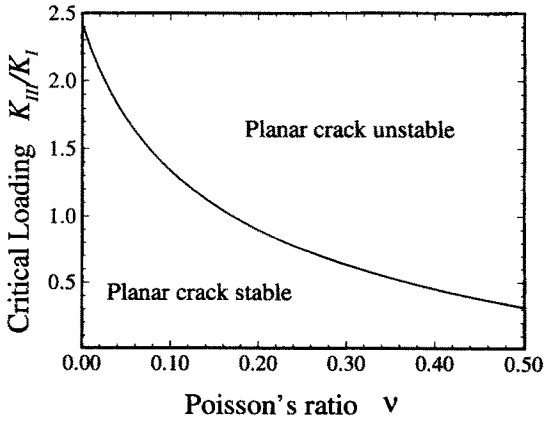

Fig. 7. Critical loading for a mode I/mode III crack to develop a wavy profile.

$$\left(\frac{K_I^\infty}{2} - 2T_{22}\sqrt{\frac{2a}{\pi}}\right)\gamma = 0, \quad (J_{21}(v, ak)K_I^\infty - \sqrt{2/k}T_{22}S_{222}(v, ak))\omega \sin ks = 0. \quad (47)$$

The condition $\mathcal{G}$ = constant on the propagating crack is satisfied automatically. For $T_{22} < 0$, eqn (47) has only the trivial solution $\gamma = \omega = 0$, so the crack must propagate along a planar path. For $T_{22} > 0$, it is always possible to find values of a and k which allow γ and ω to be non-zero. Under these conditions, the crack may kink or it may begin to propagate along a wavy path. We conclude that $T_{22} < 0$ is a necessary condition for planar mode I crack growth to be stable. The same result has been found by several authors, using two-dimensional perturbation methods.

Following an identical argument, one may show that the T-stress component T_{33} plays a similar role in initiating non-planar crack growth. If $T_{33} < 0$, the crack must remain in its original plane in order to satisfy $K_{II} = 0$ at all points on the crack front. If $T_{33} > 0$, a wavy kink may form at the crack tip so that planar crack growth is unstable. In the same way, the influence of T_{23} may be found. It is evident from eqn (29) that for a pure mode I crack, no combination of parameters in the perturbation can satisfy the criterion $K_{II} = 0$, irrespective of the magnitude of T_{23}. This suggests that the crack is likely to propagate in its initial plane for all values of T_{23}.

We conclude this section with some comments on the limitations of our stability analysis. Our predictions were made by assuming a particular geometry for the kink forming at the tip of the semi-infinite crack. It was assumed that the crack was likely to deviate from its initial plane if any non-planar kink could be found which satisfied appropriate fracture criteria along the crack front. There are two shortcomings of this approach. Strictly, in addition to finding an appropriate kinked crack configuration, one should show that the crack can find a path which reaches the final configuration and satisfies the fracture criteria during all stages of growth. Secondly, we examined only a limited range of possible geometries for the kink at the crack tip. That we were unable to find a kink within this range which satisfies the fracture criteria does not necessarily imply that no such kink configuration exists. Nevertheless, our predictions are in good agreement with more rigorous analyses for two-dimensional cracks, and are also confirmed by the full scale numerical simulations described in the next section.

7. NUMERICAL SIMULATIONS OF NON-PLANAR CRACK GROWTH

Our perturbation solution predicts the combination of remote loads which causes a planar semi-infinite crack to deviate from its initial plane. However, it gives little indication of the path followed by the crack during non-planar growth. We address this issue here, using a full numerical analysis. Several authors have investigated the two-dimensional problem of a crack propagating under mixed mode I/mode II loading or under the T-stress component T_{22}. We therefore restrict our attention to cracks propagating under mixed mode I/mode III loads, or subjected to a remote T_{33} stress component.

The problem to be solved is illustrated in Fig. 3. A semi-infinite crack is subjected to remote loading. In order to initiate unstable non-planar growth, we assume that the initial crack has a small imperfection which causes it to deviate from the (x_2, x_3) plane. The height $A(x_2, x_3)$ of the crack above the plane is chosen to be

$$A(x_2, x_3) = \begin{cases} (x_2 + a)\omega[\cos(kx_3) + \varepsilon \cos(kx_3/2) + \varepsilon^2 \cos(kx_3/4)], & x_2 > -a \\ 0 & x_2 < -a. \end{cases} \quad (48)$$

Values of $\omega = 0.1\pi/180$, $ak = \pi/2$, $\varepsilon = 0.25$ and $\nu = 0.25$ were used in the simulations reported here. The crack is subjected to far-field loading, parameterized by K_I^∞, K_{III}^∞ and T_{33}. It is assumed that the crack propagates so that $K_{II} = 0$ and $\mathcal{G} = \mathcal{G}_c$ at all points on the local crack tip, where $\mathcal{G}_c$ is the fracture toughness of the solid. Crack growth is simulated by adding successive increments in length to the crack. During each increment, the crack

is assumed to extend so that a point at s on the crack front advances a distance $\delta a(s)$, at an angle $\omega(s)$ to the current crack tip. The crack advance δa and angle ω are chosen by iteration to satisfy the fracture criteria. For each iteration, the stress intensity factors are calculated using the numerical outlined in Section 4. Once a convergent solution has been found, the crack is re-meshed, a new increment in crack length is added, and the process is repeated.

The results of our simulations are shown in Figs 8–10. Figures 8 and 9 show the path followed by a crack subjected to mixed mode I/mode III loads, for two values of $K_{III}^{\infty}/K_{I}^{\infty}$. Figure 8 is a three-dimensional view of the crack surface. To show the rate of growth of

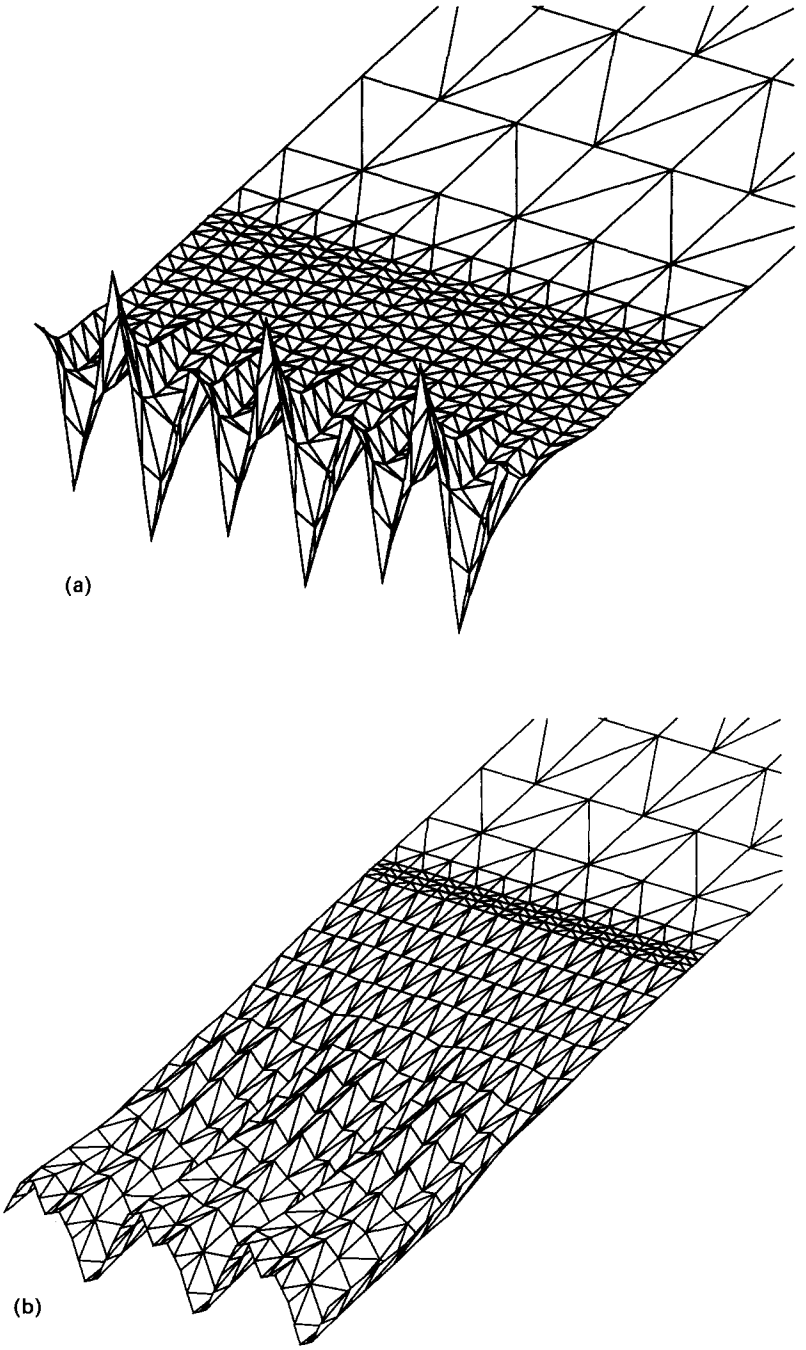

Fig. 8. The path of an initially planar semi-infinite crack subjected to mode I/mode III loads. Note that the out-of-plane displacement of the crack faces is magnified 150 times. (a) $K_{III}/K_{I} = 2$; (b) $K_{III}/K_{I} = 0.2$.

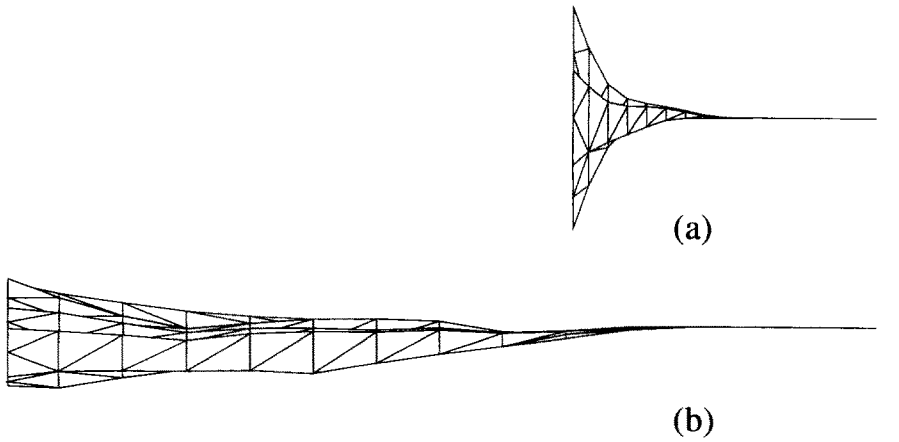

Fig. 9. A view along the x_3 axis of the cracks shown in Fig. 8. The out-of-plane displacement of the crack is magnified 150 times.

the amplitude of the waviness of the crack, a view of both cracks along the x_3 axis is drawn in Fig. 9. In each figure, the out-of-plane displacement of the crack faces has been magnified 150 times, to show clearly the nature of the crack path. The amplitude of the waviness of the crack faces is therefore greatly exaggerated. The loading applied to the crack shown in Fig. 8(a) is in the regime where unstable non-planar crack growth is predicted. As expected, the amplitude of the initial waviness of the crack grows exponentially as the crack propagates. The higher frequency components of the initial perturbation grow less rapidly than the low frequency ones, and the low frequency terms eventually dominate. The wavelength of the roughness of the crack faces therefore appears to increase as the crack grows. The pattern of fracture is remarkably close to the experimental observations reported by Sommer (1969). It should be noted that we have restricted our numerical analyses to conditions

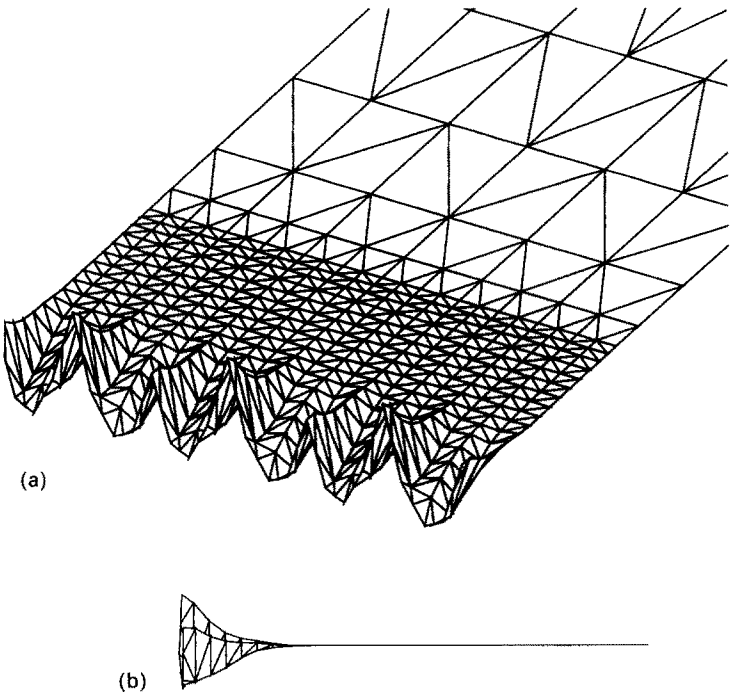

Fig. 10. The path of an initially planar mode I semi-infinite crack subjected to remote T_{33}, for $T_{33}\sqrt{\omega a}/K_I^{\infty} = 0.75$. (a) Three-dimensional view; (b) view along x_3 axis. The out-of-plane displacement of the crack has been magnified 150 times in each figure.

where the faces of the crack do not contact. In most practical situations, the crack propagates far enough to ensure that the roughness of the crack faces exceeds the crack opening displacements. The crack faces then touch, and the fracture process is considerably more complicated than the cases we consider here.

A contrasting result is shown in Figs 8(b) and 9(b). In this case, the crack is subjected to mode I/mode III loads, with the ratio $K_{III}^{\infty}/K_{I}^{\infty} = 0.2$. This combination of loads is in the regime were stable planar growth is predicted. Under these conditions, the amplitude of the perturbation in crack geometry grows very slowly. At the same time, high frequency components of waviness tend to die out, so that the roughness of the crack faces decreases as the crack grows. Eventually, the crack returns to a planar configuration, confirming the predictions of the stability analysis given in the preceding section.

Finally, Fig. 10 shows the behavior of a mode I crack subjected to a positive T_{33}, with a magnitude $T_{33}\sqrt{\omega a}/K_{I}^{\infty} = 0.75$, where a and ω are the parameters governing the amplitude of the initial imperfection in the crack geometry defined in eqn (48). Under this loading, the planar crack configuration is unstable. As expected, the numerical simulations show that the waviness of the cracked plane increases as the crack grows. Qualitatively, the nature of the fracture surface is similar to the results obtained for mixed mode I/mode III cracks; the low frequency terms in the initial imperfection grow more rapidly than high frequency ones, so that the wavelength of the roughness appears to increase as the crack grows.

8. CONCLUSIONS

A perturbation method has been developed for calculating stress intensity factors for slightly non-planar cracks. The method reduces the non-planar crack problem to an equivalent one, involving a planar reference crack loaded by a fictitious distribution of tractions on its faces. Expressions for the effective tractions were calculated by perturbing the integral equation governing the opening displacements on a planar crack. The method was used to calculate stress intensity factors for slightly wavy semi-infinite cracks subjected to remote loading. For the particular case where the crack has no waviness in a direction parallel to the crack front, we recovered the two-dimensional solutions derived by Cotterell and Rice (1980). However, our results do not agree with the predictions of an alternative perturbation method derived by Gao (1992). The cause of this discrepancy is discussed in Appendix A. To investigate the range of validity of our perturbation solution, we have compared its predictions to full numerical solutions. It was shown that the perturbation solution is accurate even for relatively large deviations of the crack from a planar configuration. In principle, our analysis could also be used to calculate stress intensity factors for slightly non-planar penny shaped cracks, although it would be a formidable undertaking to evaluate some of the integrals involved in the solution.

The perturbation scheme was used to predict the path followed by an initially planar semi-infinite crack subjected to remote loads. It was shown that three general types of crack propagation may occur. For some combinations of remote loads, the crack remains in its initial plane. Alternatively, it may kink and propagate at an angle to the initial crack. Finally, in some circumstances the crack may propagate along a wavy path, such that the macroscopic fracture surface remains co-planar with the initial crack, but the crack front deviates from the (x_2, x_3) plane and leaves a rough fracture surface in the wake of the crack. For a crack subjected to mixed mode I/mode II loading, it was shown that the crack will always kink if $K_{II} \neq 0$, but is unlikely to develop a wavy profile. A crack subjected to mixed mode I/mode III loads develops a wavy profile if the ratio K_{III}/K_{I} exceeds a critical value. The critical ratio is shown as a function of Poisson's ratio in Fig. 7. The role of T-stresses in governing the path of a mode I crack was also investigated. A positive T-stress in a direction perpendicular to the crack front (T_{22} in Fig. 3) may cause the crack to kink or develop a wavy profile. A positive T-stress parallel to the crack front (T_{33}) causes the crack to develop a wavy profile. The component T_{23} appears to have no affect on the crack path.

Finally, we have used a numerical technique to calculate the path of a crack propagating under mixed mode remote loading. The results confirm the predictions of our stability

analysis. In addition, the predicted crack path closely resembles experimental observations reported in the literature.

Acknowledgements—This work was supported by the Materials Research Group on Micromechanics of Failure Resistant Materials at Brown University, which is funded by the National Science Foundation under Grant No. DMR-9223683. The Office of Naval Research supported the initial stages of work through Grant No. N00014-90-J-1758.

REFERENCES

Banichuk, N. V. (1970). Determination of the form of curvilinear crack by small parameter technique. *Izv. An. SSR MTT* **7** 2, 130–137.

Bueckner, H. F. (1970). A novel principle for the computation of stress intensity factors. *ZAMM* **50,** 529–546.

Cotterell, B. (1965). On brittle fracture paths. *Int. J. Fract.* **1,** 96–103.

Cotterell, B. and Rice, J. R. (1980). Slightly curved or kinked cracks. *Int. J. Fract.* **16**(2), 155.

Erdogan, F. and Sih, G. C. (1963). On the crack extension in plates under plane loading and transverse shear. *J. Basic Engng* **85,** 519–527.

Ewing, P. D. and Williams, J. G. (1974). Further observations on the angled crack problem. *Int. J. Fract.* **10,** 135.

Ewing, P. D., Swedlow, J. L. and Williams, J. G. (1976). Further results on the angled crack problem. *Int. J. Fract.* **12,** 85–93.

Faber, K. T. and Evans, A. G. (1983). Crack deflection processes I: Theory. *Acta Met.* **31**(4), 577–584.

Fares, N. (1989). Crack fronts trapped by arrays of obstacles: numerical solutions based on a surface integral representation. *J. Appl. Mech.* **56,** 837–843.

Fleck, N. A. (1991). Brittle fracture due to an array of microcracks. *Proc. R. Soc. London* **432A,** 55–76.

Finnie, I. and Saich, A. (1973). A note on the angled crack problem and the directional stability of cracks. *Int. J. Fract.* **9,** 484–486.

Gao, H. (1992). Three-dimensional slightly nonplanar cracks. *J. Appl. Mech.* **59,** 335–343.

Gao, H. and Rice, J. R. (1986). Shear stress intensity factors for a planar crack with slightly curved front. *J. Appl. Mech.* **53,** 774.

Goldstein, R. V. and Sagalnik, R. L. (1974). Brittle fracture of solids with arbitrary cracks. *Int. J. Fract.* **10,** 507–523.

Karihaloo, B. L., Keer, L. M., Nemat-Nasser, S. and Oranratnachai, A. (1981). Approximate description of crack kinking and curving. *J. Appl. Mech.* **48,** 515–519.

Kassir, M. K. and Sih, G. C. (1973). Application of Papkovich–Neuber potentials to a crack problem. *Int. J. Solids Structures* **9,** 643–645.

Palaniswamy, K. and Knauss, W. G. (1978). On the problem of crack extension in brittle solids under general loading. In *Mechanics Today* (Edited by S. Nemat-Nasser), Vol. 4, pp. 87–148. Pergamon Press, Oxford.

Radon, C. C., Lever, P. S. and Culver, L. E. (1977). Fracture toughness of PMMA under biaxial stress. In *Fracture*, Vol. 3, pp. 1113–1118. UW Press.

Rice, J. R. (1985). First order variations in elastic fields due to variation in location of a planar crack front. *J. Appl. Mech.* **52,** 571–579.

Sih, G. C. (1973). Some basic problems in fracture mechanics. *Engng Fract. Mech.* **5,** 365–377.

Sih, G. C. (1974). Strain energy density factor applied to mixed mode crack problems. *Int. J. Fract.* **10,** 305–21.

Sommer, E. (1969). Formation of fracture lances in glass. *Engng Fract. Mech.* **1,** 539–546.

Sumi, Y., Nemat-Nasser, S. and Keer, L. M. (1983). On crack branching and curving in a finite body. *Int. J. Fract.* **21,** 67–79.

Suresh, S. and Tschegg, E. K. (1987). Combined mode I–mode III fracture of fatigue precracked alumina. *J. Am. Ceram. Soc.* **70**(10), 726–733.

Suresh, S., Shih, C. F., Morrone, A. and O'Dowd, N. P. (1990). Mixed-mode fracture toughness of ceramic materials. *J. Am. Ceram. Soc.* **73**(5), 1257–1267.

Tschegg, E. K. and Suresh, S. (1988). Mode III fracture of 4340 steel: effects of tempering temperature and fracture surface interference. *Met. Trans.* **19A,** 3035.

Ulfyand, Y. S. (1965). Survey of articles on the application of integral transforms in the theory of elasticity. North Carolina State University, Department of Applied Mathematics Research Group. File No. PSR 24/6. Raleigh, NC.

Williams, J. G. and Ewing, P. D. (1972). Fracture under complex stress—the angle crack problem. *Int. J. Fract.* **8,** 441–446.

Xu, G. and Ortiz, M. (1993). A variational boundary integral method for the analysis of 3-D cracks of arbitrary geometry modeled as continuous distributions of dislocation loops. *Int. J. Num. Meth. Engng* **36,** 3675.

APPENDIX A

A first-order estimate of the stress intensity factors for slightly wavy three-dimensional cracks has been found by Gao (1992), using an alternative perturbation method. Since our solution does not agree with his, we investigate the difference between the two approaches in more detail in this appendix. We begin by summarizing Gao's derivation. Suppose that an infinite solid contains a crack which lies on a slightly wavy surface $\hat{S}$. For simplicity, assume that the loading consists of a remote stress $\boldsymbol{\sigma}^{\infty}$, and that the crack faces are traction free. We wish to calculate the state of stress $\hat{\boldsymbol{\sigma}}$ which surrounds the wavy crack. As a starting point, imagine that the stress field induced by this loading is known for a planar crack, lying on a surface S, which is the projection of $\hat{S}$ on the

x_2, x_3 plane. Denote this solution by $\boldsymbol{\sigma}$. We now pose the following question; what additional tractions $\mathbf{t}^{\text{eff}}$ should one distribute on the planar crack faces, in order to free the surface $\hat{S}$ from tractions?

Gao calculates the effective tractions by introducing a perturbation expansion of the state of stress $\boldsymbol{\sigma}$. To this end, let the state of stress around the wavy crack be

$$\hat{\boldsymbol{\sigma}}(x_1, x_2, x_3) = \boldsymbol{\sigma}(x_1, x_2, x_3) + \delta\boldsymbol{\sigma}(x_1, x_2, x_3), \tag{A1}$$

where $\delta\boldsymbol{\sigma}$ is a small correction to $\boldsymbol{\sigma}$ introduced to satisfy the boundary conditions on $\hat{S}$. On the wavy surface $\hat{S}$, one has

$$\hat{\boldsymbol{\sigma}} = \boldsymbol{\sigma}(0, x_2, x_3) + \frac{\partial \boldsymbol{\sigma}(0, x_2, x_3)}{\partial x_1}\,\delta z(x_2, x_3) + \delta\boldsymbol{\sigma}(0, x_2, x_3) + \mathcal{O}(\delta z^2), \tag{A2}$$

where δz is the height of $\hat{S}$ above S. The boundary conditions on $\hat{S}$ are

$$\hat{\boldsymbol{\sigma}}\hat{\mathbf{n}} = 0 \tag{A3}$$

where $\hat{\mathbf{n}} = \mathbf{e}_1 - \delta z_{,2}\mathbf{e}_2 - \delta z_{,3}\mathbf{e}_3$ is the normal to $\hat{S}$, $\mathbf{e}_i$ being the basis vectors. Substituting eqn (A2) into eqn (A3), using $\boldsymbol{\sigma}(0, x_2, x_3)\mathbf{e}_1 = 0$ and neglecting second-order terms in δz, one finds that

$$\delta\boldsymbol{\sigma}(0, x_2, x_3)\mathbf{e}_1 = \boldsymbol{\sigma}(0, x_2, x_3)[\delta z_{,2}\mathbf{e}_2 + \delta z_{,3}\mathbf{e}_3] - [\delta z \boldsymbol{\sigma}_{,1}]\mathbf{e}_1. \tag{A4}$$

We now interpret eqn (A4) as boundary conditions on the (x_2, x_3) plane for the stress state $\delta\boldsymbol{\sigma}$. The right hand side of eqn (A4) is therefore the distribution of effective tractions acting on the planar reference crack.

We may compare this result with our expression for the effective tractions in eqn (11). Note first that for a planar reference crack, the last integral in eqn (11) vanishes. From eqn (1) it is evident that

$$\boldsymbol{\sigma}(0, x_2, x_3)[\delta z_{,2}\mathbf{e}_2 + \delta z_{,3}\mathbf{e}_3] \equiv [\boldsymbol{\sigma}^{\infty}]\delta\mathbf{n} + \int_S [\mathbf{F}(\boldsymbol{\xi}, \mathbf{x})\nabla\mathbf{u}(\boldsymbol{\xi})]\delta\mathbf{n}(\mathbf{x})\,\mathrm{d}A. \tag{A5}$$

Differentiating eqn (1), one finds that

$$[\delta z \boldsymbol{\sigma}_{,1}]\mathbf{e}_1 \equiv [\nabla\boldsymbol{\sigma}^{\infty}\delta\mathbf{x}]\mathbf{n}(\mathbf{x}) + \int_S \left[\delta z(\mathbf{x})\frac{\partial \mathbf{F}(\boldsymbol{\xi}, \mathbf{x})}{\partial x_1}\nabla\mathbf{u}(\boldsymbol{\xi})\right]\mathbf{n}(\mathbf{x})\,\mathrm{d}A. \tag{A6}$$

The integral in eqn (A6) must be interpreted with some care; it is undefined if $\mathbf{x}$ lies on S and must be evaluated by taking the limit as $\mathbf{x}$ approaches the crack faces. This reflects the fact that some components of the stress field surrounding a crack may be discontinuous across the cracked surface. Finally, using eqn (9) one finds that our expression for the effective tractions given in eqn (11) contains an additional term which is not present in eqn (A4). This term is given by

$$\int_S \left[\delta z(\boldsymbol{\xi})\frac{\partial \mathbf{F}(\boldsymbol{\xi}, \mathbf{x})}{\partial \xi_1}\nabla\mathbf{u}(\boldsymbol{\xi})\right]\mathbf{n}(\mathbf{x})\,\mathrm{d}A_{\xi}. \tag{A7}$$

To understand the cause of the discrepancy between Gao's solution and ours, it is instructive to interpret the physical significance of this term. Note that

$$\boldsymbol{\sigma}(\mathbf{x}) = \int_S \mathbf{F}(\boldsymbol{\xi}, \mathbf{x})\nabla\mathbf{u}(\boldsymbol{\xi})\,\mathrm{d}A_{\xi} \tag{A8}$$

represents the state of stress $\boldsymbol{\sigma}$ at a point $\mathbf{x}$, induced by the displacement jump distribution $\mathbf{u}(\boldsymbol{\xi})$ across the planar surface S. Now, suppose that we move the same displacement jump from S to the new surface $\hat{S}$. This changes the stress at $\mathbf{x}$ by an amount

$$\delta\boldsymbol{\sigma}(\mathbf{x}) = \int_S \mathbf{F}(\hat{\boldsymbol{\xi}}, \mathbf{x})\nabla\mathbf{u}(\hat{\boldsymbol{\xi}})\,\mathrm{d}A_{\hat{\xi}} - \int_S \mathbf{F}(\boldsymbol{\xi}, \mathbf{x})\nabla\mathbf{u}(\boldsymbol{\xi})\,\mathrm{d}A_{\xi}, \tag{A9}$$

where $\hat{\boldsymbol{\xi}} = \boldsymbol{\xi} + \delta z(\boldsymbol{\xi})\mathbf{e}_1$. One may expand eqn (A9) to first-order in δz, with the result

$$\delta\boldsymbol{\sigma}(\mathbf{x}) = \int_S \left[\delta z(\boldsymbol{\xi})\frac{\partial \mathbf{F}(\boldsymbol{\xi}, \mathbf{x})}{\partial \xi_1}\nabla\mathbf{u}(\boldsymbol{\xi})\right]\mathrm{d}A_{\xi} + \mathcal{O}(\delta z^2). \tag{A10}$$

Thus, we see that the additional term in our solution represents the effect of moving the opening displacements $\mathbf{u}(\boldsymbol{\xi})$ from the planar surface S to the wavy surface $\hat{S}$.

This shows that if one interprets Gao's derivation as a strict superposition of two equilibrium stress states, the derivation does not give the stress field around a wavy crack subjected to remote loading. Instead, his solution represents a *planar* crack, which is subjected to a combination of remote loading together with an additional distribution of traction on its faces. The additional distribution of traction happens to free the wavy surface $\hat{S}$ from stress. There is a subtle difference between this solution and the correct solution to a wavy crack under remote loading. In the correct solution, there should be a displacement jump across the wavy surface $\hat{S}$, and the solution should contain no discontinuities in traction. In Gao's solution, the displacement jump seems to occur

across the planar surface S. In addition, if one calculates the effective tractions using Gao's expressions, one finds that the tractions have different values on the upper and lower crack faces. Therefore, his solution also appears to contain an inadmissible traction jump across S.

One may develop a construction somewhat similar to Gao's, which would lead to our expressions for effective tractions. It begins with the solution to a planar crack subjected to remote loading. Let $\mathbf{u}(\xi)$ denote the opening displacements for the planar crack. Next, we move the same opening displacements to the wavy surface $\hat{S}$. This step does not appear in Gao's derivation. Moving the opening displacements causes a change in stress, which may be calculated using eqn (A10). The new stress distribution does not satisfy the boundary conditions on the wavy crack faces. Therefore, one must distribute additional tractions over the crack faces in order to free them from normal and tangential stress. The tractions are given by the sum of eqn (A4) and the additional term in eqn (A7). Finally, to compute stress intensity factors for the wavy crack, one may assume that the wavy crack has the same crack face weight functions as the planar reference crack, accurate to first-order in δz. Therefore, the change in stress intensity factors follow from eqn (4). This approach leads to the results we gave in Section 2.

Finally, we note that the preceding discussion has shown only that Gao's expressions for effective tractions differ from our results. This does not necessarily imply that the two methods give different results for stress intensity factors on the wavy crack. In fact, for the particular case of a two-dimensional perturbation of a semi-infinite crack, given in eqns (22) *et seq.*, both methods give identical results. The examples given in Section 3 show that for fully three-dimensional perturbations, the two methods do lead to different expressions for stress intensity factors. The results of the full-field numerical simulations which we reported in Section 4 give encouraging support for the results we derive in this paper. However, the slightly non-planar 3D crack problem would be worthy of further study to clarify the differences between Gao's results and ours.

APPENDIX B: CALCULATING STRESS INTENSITIES FOR A WAVY SEMI-INFINITE CRACK

Here we describe in detail the steps leading to eqns (16)–(19) which give the stress intensity factors for a slightly wavy semi-infinite crack. There are some difficulties in interpreting the nature of the remote loading applied to a semi-infinite crack. To avoid these difficulties, we imagine perturbing a large slit crack which lies in the region $\{x_1 = 0, -c < x_2 < 0 - \infty < x_3 < \infty\}$ (Fig. B1). Far from the crack, the solid is subjected to a uniform state of stress. We assume that the loading induces stress intensity factors K_{I}^{∞}, K_{II}^{∞} and $K_{\mathrm{III}}^{\infty}$ on the planar slit crack. Therefore,

$$\sigma_{11}^{\infty} = \sqrt{\frac{2}{\pi c}} K_{\mathrm{I}}^{\infty}, \quad \sigma_{12}^{\infty} = \sqrt{\frac{2}{\pi c}} K_{\mathrm{II}}^{\infty}, \quad \sigma_{13}^{\infty} = \sqrt{\frac{2}{\pi c}} K_{\mathrm{III}}^{\infty}. \tag{B1}$$

In addition, the solid may be subjected to T-stress components, which we denote by

$$\sigma_{22}^{\infty} = T_{22}, \quad \sigma_{33}^{\infty} = T_{33} + \nu \sqrt{\frac{2}{\pi c}} K_{\mathrm{I}}^{\infty}, \quad \sigma_{23}^{\infty} = T_{23}. \tag{B2}$$

The second eqn of (B2) has been written so that if $T_{ij} = 0$, the solid deforms in a state of plane strain. The loading induces opening displacements on the slit crack which are given by

$$\begin{aligned} u_1 &= \frac{4(1-\nu)}{\mu} \frac{K_{\mathrm{I}}}{\sqrt{2\pi}} \sqrt{-x_2(1+x_2/c)}, \\ u_2 &= \frac{4(1-\nu)}{\mu} \frac{K_{\mathrm{II}}}{\sqrt{2\pi}} \sqrt{-x_2(1+x_2/c)}, \\ u_3 &= \frac{4}{\mu} \frac{K_{\mathrm{III}}}{\sqrt{2\pi}} \sqrt{-x_2(1+x_2/c)}. \end{aligned} \tag{B3}$$

Now, suppose that the slit crack is perturbed slightly from its planar configuration. Assume that the crack is perturbed only in the region $\{-a \leqslant x_2 \leqslant 0, -\infty < x_3 < \infty\}$ so that a point at $(0, x_2, x_3)$ within this region is displaced to $(\delta z, x_2, x_3)$. The rest of the crack is assumed to remain planar. We now apply the procedure outlined in Section 2 to calculate the change in stress intensity factors $\delta K_s(s)$ at a point s on the perturbed crack front.

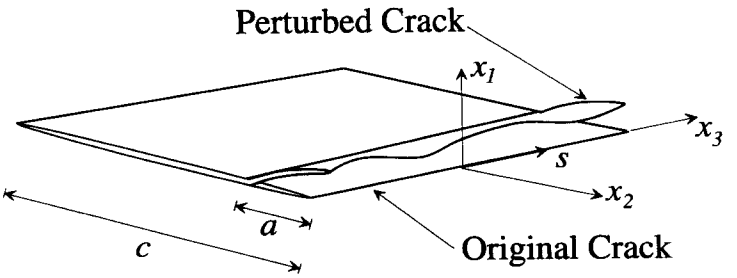

Fig. B1. A planar slit crack which is perturbed to a wavy configuration near one tip.

The first step is to rotate and translate the planar crack so that it is tangent to the perturbed crack at the point s. The required translation is $\mathbf{d} = \delta z[\mathbf{x}(s)]\mathbf{e}_1$, while the rotation is $\boldsymbol{\omega} = \gamma\mathbf{e}_2 + \omega\mathbf{e}_3$, where $\omega = \delta z_{,2}[\mathbf{x}(s)]$ and $\gamma = \delta z_{,3}[\mathbf{x}(s)]$. Translating the crack causes no change in the stress intensity factors, while rotating it is equivalent to rotating the remote stress field through an equal and opposite angle. Thus, the change in stress intensity factors caused by setting up the reference crack is

$$\begin{aligned}
\delta K_{\mathrm{I}}^{\mathrm{rot}} &= -2\omega K_{\mathrm{II}}^{\infty} - 2\gamma K_{\mathrm{III}}^{\infty},\\
\delta K_{\mathrm{II}}^{\mathrm{rot}} &= \omega K_{\mathrm{I}}^{\infty} - (\omega T_{22} + \gamma T_{23})\sqrt{\pi c/2},\\
\delta K_{\mathrm{III}}^{\mathrm{rot}} &= (1-\nu)\gamma K_{\mathrm{I}}^{\infty} - (\omega T_{23} + \gamma T_{33})\sqrt{\pi c/2}.
\end{aligned} \tag{B4}$$

Next, the reference crack is subjected to a second perturbation so as to reach the required geometry. The additional perturbation δz^{ref} is given by

$$\delta z^{\mathrm{ref}}(\mathbf{x}) = \delta z(\mathbf{x}) - \delta z[\mathbf{x}(s)] - x_2\omega - x_3\gamma. \tag{B5}$$

The change in stress intensity factors due to this perturbation must be calculated by evaluating the effective tractions using eqn (11), and then substituting into eqn (4). We will evaluate each integral in eqn (11) in turn. Note first that for a uniform state of remote stress, the first term in eqn (11) vanishes. To evaluate the second and third terms, note that

$$\boldsymbol{\sigma}(\mathbf{x}) = \boldsymbol{\sigma}^{\infty} + \int_S \mathbf{F}(\boldsymbol{\xi}, \mathbf{x})\nabla\mathbf{u}(\boldsymbol{\xi})\,\mathrm{d}A_{\xi} \tag{B6}$$

represents the stress $\boldsymbol{\sigma}$ at a point $\mathbf{x}$ in a solid containing the unperturbed crack, by eqn (1). The stresses on the faces of the slit crack may be found from the exact solution to this problem, and are

$$\begin{aligned}
\sigma_{22}^{\pm} &= -K_{\mathrm{I}}^{\infty}\sqrt{\frac{2}{\pi c}} \mp K_{\mathrm{II}}^{\infty}\sqrt{\frac{2}{\pi x}}\frac{2(x_2 + c/2)}{\sqrt{-x_2(x_2+c)}} + T_{22},\\
\sigma_{33}^{\pm} &= -\nu K_{\mathrm{I}}^{\infty}\sqrt{\frac{2}{\pi c}} \mp \nu K_{\mathrm{II}}^{\infty}\sqrt{\frac{2}{\pi c}}\frac{2(x_2 + c/2)}{\sqrt{-x_2(x_2+c)}} + T_{33},\\
\sigma_{23}^{\pm} &= \mp K_{\mathrm{III}}^{\infty}\sqrt{\frac{2}{\pi c}}\frac{(x_2 + c/2)}{\sqrt{-x_2(x_2+c)}} + T_{23}.
\end{aligned} \tag{B7}$$

All the remaining components of stress are zero on the crack faces. In eqn (B7), the symbols σ^+ and σ^- have been used to denote the stresses on the upper and lower crack faces, respectively. Noting that $\delta\mathbf{n}(\mathbf{x}) = -\delta z_{,2}^{\mathrm{ref}}(\mathbf{x})\mathbf{e}_2 - \delta z_{,3}^{\mathrm{ref}}(\mathbf{x})\mathbf{e}_3$ for the planar crack, we find that the second and third terms in eqn (11) give rise to the following contribution to the effective tractions

$$\begin{aligned}
t_1(\mathbf{x}) &= 0,\\
t_2^{\pm}(\mathbf{x}) &= -\delta z_{,2}^{\mathrm{ref}}(\mathbf{x})\sigma_{22}^{\pm} - \delta z_{,3}^{\mathrm{ref}}(\mathbf{x})\sigma_{23}^{\pm},\\
t_3^{\pm}(\mathbf{x}) &= -\delta z_{,2}^{\mathrm{ref}}(\mathbf{x})\sigma_{23}^{\pm} - \delta z_{,3}^{\mathrm{ref}}(\mathbf{x})\sigma_{33}^{\pm}.
\end{aligned} \tag{B8}$$

Here, we have used t_i^+ and t_i^- to denote the tractions acting on the upper and lower crack faces, respectively.

Next, consider the contribution to $\mathbf{t}^{\mathrm{eff}}$ from the second integral in eqn (11). For a planar slit crack with opening displacements given by eqn (B3), the integrals may be reduced to the following form

$$\begin{aligned}
t_i^{\pm} = {} & \frac{K_{\mathrm{I}}^{\infty}}{(2\pi)^{3/2}}\lim_{r_1\to\pm 0}\int_S \frac{M(\xi_2)}{R^3}(\delta z^{\mathrm{ref}}(\boldsymbol{\xi}) - \delta z^{\mathrm{ref}}(\mathbf{x}))\left\{15\frac{r_i r_2 r_1^2}{R^4} - 3\frac{\delta_{i2}r_1^2}{R^2} - 3\frac{\delta_{i1}r_1 r_2}{R^2}\right\}\mathrm{d}A_{\xi}\\
& + \frac{K_{\mathrm{II}}^{\infty}}{(2\pi)^{3/2}}\lim_{r_1\to\pm 0}\int_S \frac{M(\xi_2)}{R^3}\left[(\delta z^{\mathrm{ref}}(\boldsymbol{\xi}) - \delta z^{\mathrm{ref}}(\mathbf{x}))\left\{3\frac{\delta_{i1}r_1^2}{R^2} + 9\frac{r_i r_1}{R^2} - 15\frac{r_i r_1^3}{R^4}\right.\right.\\
& \left. - 3(1-\nu)\frac{\delta_{i3}r_1 r_3}{R^2}\right\} + \delta z_{,3}^{\mathrm{ref}}(\boldsymbol{\xi})\left\{(2-\nu)\delta_{i3}r_1 - 3\frac{r_i r_1 r_3}{R^2}\right\}\left.\right]\mathrm{d}A_{\xi}\\
& + \frac{K_{\mathrm{III}}^{\infty}}{(2\pi)^{3/2}}\frac{(1-2\nu)}{(1-\nu)}\lim_{r_1\to\pm 0}\int_S \frac{M(\xi_2)}{R^3}\left[3(1-\nu)(\delta z^{\mathrm{ref}}(\boldsymbol{\xi}) - \delta z^{\mathrm{ref}}(\mathbf{x}))\delta_{i3}\frac{r_1 r_2}{R^2}\right.\\
& \left. - \delta z_{,3}^{\mathrm{ref}}\left\{(2-\nu)r_1\delta_{i2} - 3\frac{r_i r_1 r_2}{R^2}\right\}\right]\mathrm{d}A_{\xi}\\
& + \frac{K_{\mathrm{I}}^{\infty}}{(2\pi)^{3/2}}\int_S \frac{M(\xi_2)}{R^3}\left\{[\delta z^{\mathrm{ref}}(\boldsymbol{\xi}) - \delta z^{\mathrm{ref}}(\mathbf{x})]\left(\delta_{i2} - \frac{3r_2(\delta_{i2}r_2 - \delta_{i3}r_3)}{R^2}\right)\right.\\
& \left. - (1-\nu)\delta z_{,3}^{\mathrm{ref}}(\boldsymbol{\xi})(r_2\delta_{i3} - r_3\delta_{i2})\right\}\mathrm{d}A_{\xi}
\end{aligned}$$

$$-\frac{K_{II}^{\infty}}{(2\pi)^{3/2}}\int_S \frac{\delta_{i1}M(\xi_2)}{R^3}\{\delta z^{ref}(\xi)-\delta z^{ref}(\mathbf{x})+(1-2\nu)r_3\delta z^{ref}_{,3}(\xi)\}\,dA_\xi$$

$$+\frac{K_{III}^{\infty}(1-2\nu)}{(2\pi)^{3/2}(1-\nu)}\int_S \frac{\delta_{i1}r_2\delta z^{ref}_{,3}(\xi)M(\xi_2)}{R^3}\,dA_\xi, \tag{B9}$$

where δ_{ij} denotes the Kronecker delta and

$$r_i = x_i-\xi_i,\quad R=\sqrt{r_ir_i},\quad M(\xi_2)=\frac{(1+2\xi_2/c)}{\sqrt{-\xi_2(1+\xi_2/c)}}. \tag{B10}$$

In eqn (B9), the first three integrals have different values on the upper and lower crack faces, and must be evaluated by taking their limit as $r_1\to\pm 0$. In the remaining integrals, one may set $r_1=0$ before integration, provided that Cauchy Principal Values are taken.

The first three integrals in eqn (B9) may be evaluated explicitly, using the following procedure. Note that as $r_1\to 0$, each of the first three integrands becomes singular, with a singularity of order $1/R^2$ as $\xi\to\mathbf{x}$. It is convenient to extract the singular part of each integral as follows;

$$\int_S G(\mathbf{x},\xi)\,dA_\xi=\int_{S-\rho}G(\mathbf{x},\xi)\,dA_\xi+\int_\rho G(\mathbf{x},\xi)\,dA_\xi, \tag{B11}$$

where $G(\mathbf{x},\xi)$ has been used to denote the integrand and ρ is a small region surrounding the singular point at $\mathbf{x}$. The shape of this region is arbitrary; a small square around $\mathbf{x}$ such that $\{\xi_1=0,\ -\varepsilon\leqslant\xi_2-x_2\leqslant+\varepsilon,\ -\varepsilon\leqslant\xi_3-x_3\leqslant+\varepsilon\}$ is a convenient choice. Now, the integrals over the region $S-\rho$ are regular, so one may let $r_1\to 0$ in the integrands before integration. The integrals over $S-\rho$ therefore vanish. To evaluate the integrals over ρ, we expand $\delta z^{ref}(\xi)$ and its derivatives in a Taylor series about $\mathbf{x}$, so that, for example,

$$\delta z^{ref}(\xi)=\delta z^{ref}(\mathbf{x})-r_2\delta z^{ref}_{,2}(\mathbf{x})-r_3\delta z^{ref}_{,3}(\mathbf{x})+\cdots \tag{B12}$$

After substituting this approximation into the first three integrals in eqn (B9), the integrals over ρ may be evaluated explicitly. Then, we let $r_1\to 0$ in the resulting expressions and finally take the limit $\varepsilon\to 0$. This procedure shows that the first three integrals in eqn (B9) give rise to the following contribution to the effective tractions;

$$\begin{aligned}
t_1(\mathbf{x}) &= 0,\\
t_2^{\pm}(\mathbf{x}) &= \mp\delta z^{ref}_{,2}(\mathbf{x})\frac{K_{II}^{\infty}}{\sqrt{2\pi}}\frac{2(1+2x_2/c)}{\sqrt{-x_2(1+x_2/c)}}\mp\delta z^{ref}_{,3}(\mathbf{x})\frac{K_{III}^{\infty}}{\sqrt{2\pi}}\frac{(1+2x_2/c)}{\sqrt{-x_2(1+x_2/c)}},\\
t_3^{\pm}(\mathbf{x}) &= \mp\nu\delta z^{ref}_{,3}(\mathbf{x})\frac{K_{II}^{\infty}}{\sqrt{2\pi}}\frac{2(1+2x_2/c)}{\sqrt{-x_2(1+x_2/c)}}\mp\delta z^{ref}_{,2}(\mathbf{x})\frac{K_{III}^{\infty}}{\sqrt{2\pi}}\frac{(1+2x_2/c)}{\sqrt{-x_2(1+x_2/c)}}.
\end{aligned} \tag{B13}$$

Note that the final term in eqn (11) vanishes for a planar crack. Therefore, collecting terms from eqns (B8), (B9) and (B13), we find that the effective tractions reduce to

$$\begin{aligned}
t_1^{eff} &= \frac{-K_{II}^{\infty}}{(2\pi)^{3/2}}PV\int_S\frac{M(\xi_2)}{R^3}\left[(\delta z^{ref}(\xi)-\delta z^{ref}(\mathbf{x}))+(1-2\nu)r_3\delta z^{ref}_{,3}\right]dA_\xi\\
&\quad+\frac{K_{III}^{\infty}}{(2\pi)^{3/2}}\frac{(1-2\nu)}{(1-\nu)}PV\int_S\frac{M(\xi_2)}{R^3}r_2\delta z^{ref}_{,3}(\xi)\,dA_\xi,\\
t_2^{eff} &= \frac{K_I^{\infty}}{(2\pi)^{3/2}}PV\int_S\frac{M(\xi_2)}{R^3}\left[(\delta z^{ref}(\xi)-\delta z^{ref}(\mathbf{x}))\left(1-3\frac{r_2^2}{R^2}\right)+(1-\nu)\delta z^{ref}_{,3}(\xi)r_3\right]dA_\xi\\
&\quad+\delta z^{ref}_{,2}(\mathbf{x})K_I^{\infty}\sqrt{\frac{2}{\pi c}}-\delta z^{ref}_{,2}(\mathbf{x})T_{22}-\delta z^{ref}_{,3}(\mathbf{x})T_{23},\\
t_3^{eff} &= \frac{-K_I^{\infty}}{(2\pi)^{3/2}}PV\int_S\frac{M(\xi_2)}{R^3}\left[3(\delta z^{ref}(\xi)-\delta z^{ref}(\mathbf{x}))\frac{r_3r_2}{R^2}+(1-\nu)\delta z^{ref}_{,3}(\xi)r_2\right]dA_\xi\\
&\quad+\delta z^{ref}_{,3}(\mathbf{x})\nu K_I^{\infty}\sqrt{\frac{2}{\pi c}}-\delta z^{ref}_{,2}(\mathbf{x})T_{23}-\delta z^{ref}_{,3}(\mathbf{x})T_{33}.
\end{aligned} \tag{B14}$$

Note that the tractions now have the same value on both upper and lower crack faces.

To proceed, substitute the expression for δz^{ref} given in eqn (B5) into eqn (B14). Note that the terms involving γ and ω may be integrated explicitly. Furthermore, the contribution to $\mathbf{t}^{eff}$ due to these terms is independent of x_3. Consequently, one may find the stress intensity factor change due to these tractions by using the two-dimensional (plane strain) weight function for a slit crack. We find that the changes in stress intensity factors due to terms involving γ and ω in eqn (B14) are

$$\delta K_{\mathrm{I}}^{\omega} = \frac{\omega K_{\mathrm{II}}^{\infty}}{\pi^2} I_1 + \frac{\gamma K_{\mathrm{III}}^{\infty}}{\pi^2} \frac{(1-2\nu)}{(1-\nu)} I_1,$$

$$\delta K_{\mathrm{II}}^{\gamma\omega} = \frac{\omega K_{\mathrm{I}}^{\infty}}{\pi^2} I_1 - \frac{2\omega K_{\mathrm{I}}^{\infty}}{\pi} I_2 + (\omega T_{22} + \gamma T_{23})\sqrt{\pi c/2},$$

$$\delta K_{\mathrm{III}}^{\gamma\omega} = \frac{\nu\gamma K_{\mathrm{I}}^{\infty}}{\pi^2} I_1 - \frac{2\nu\gamma K_{\mathrm{I}}^{\infty}}{\pi} I_2 + (\omega T_{32} + \gamma T_{33})\sqrt{\pi c/2}, \tag{B15}$$

where

$$I_1 = \lim_{\beta \to 0} \int_{-c+\beta}^{-\beta} \mathrm{d}x \, \mathrm{PV} \int_{-c}^{0} \frac{(1+2\xi/c)}{(\xi - x)\sqrt{\xi x}} \frac{\sqrt{1+x/c}}{\sqrt{1+\xi/c}} \mathrm{d}\xi = \pi^2,$$

$$I_2 = \int_{-c}^{0} \sqrt{\frac{1+x/c}{-cx}} \mathrm{d}x = \frac{\pi}{2}. \tag{B16}$$

Now, if we let $\delta K_{\alpha}^{\mathrm{reg}} = \delta K_{\alpha}^{\mathrm{rot}} + \delta K_{\alpha}^{\gamma\omega}$ denote the change in stress intensity factor due to the combined effects of rotating the planar crack to a reference configuration [given in eqn (B4)], and due to evaluating the terms involving γ and ω in eqn (B14), we find that $\delta K_{\alpha}^{\mathrm{reg}}$ reduces to the expressions given in eqn (16).

Finally, we examine the terms which remain in eqn (B14) after subtracting terms containing γ and ω. These are given by eqn (B14), with δz^{ref} replaced by δz. Since $\delta z = 0$ for $\xi_2 < -a$, one may let $c \to \infty$ in the remaining terms before integration. One may then let $a \to \infty$, whereupon eqn (B14) reduces to the expression for effective tractions given in eqn (17).